**Fernando Jorge
Lopes Parente**

Efeitos cruzados em serviços sobre PON

Cross effects in services over PON

Dissertação apresentada à Universidade de Aveiro para cumprimento dos requisitos necessários à obtenção do grau de Mestre em Engenharia Electrónica e Telecomunicações, realizada sob a orientação científica do Prof. Doutor António Teixeira e do Prof. Doutor José Ferreira da Rocha, ambos do Departamento de Electrónica, Telecomunicações e Informática e do Instituto de Telecomunicações da Universidade de Aveiro.

Dedico este trabalho aos meus pais, ao meu irmão e a todos os meus amigos por todo o seu incansável e incondicional apoio e por me guiarem sempre na direcção correcta.

o júri

Presidente	Prof. Doutor Paulo Miguel Nepomuceno Pereira Monteiro
	Prof. Associado da Universidade de Aveiro
Vogal	Doutora Natasa Pavlovic
	Investigadora Sénior na Nokia Siemens Networks
Orientador	Prof. Doutor António Luís Teixeira
	Prof. Associado da Universidade de Aveiro
Co-Orienador	Prof. Doutor José Rodrigues Ferreira da Rocha
	Prof. Catedrático da Universidade de Aveiro

agradecimentos

Esta tese marca o culminar de 5 anos de trabalho na Universidade de Aveiro. Durante estes fantásticos anos, muitas foram as pessoas que me marcaram, incentivaram e ajudaram a desenvolver técnica e pessoalmente e às quais não poderia deixar de agradecer.

Quero agradecer aos meus orientadores, Prof. Dr. António Teixeira e Prof. Dr. José Ferreira da Rocha pelo apoio, orientação e troca de conhecimentos, que me ajudaram a ultrapassar as dificuldades e melhorar o meu trabalho.

Aos meus colegas de trabalho, aos projectos QREN FCT e PTin "GPON in a box", FCT "TOMAR-PON" e ao projecto Europeu do FP7 SARDANA.

Com muito orgulho por toda a experiencia de vida que me proporcionou, gostaria de deixar o meu especial agradecimento à Universidade de Aveiro, em particular ao Departamento de Electrónica, Telecomunicações e Informática e ao Instituto de Telecomunicações.

Aos elementos da equipa de Futsal Feminino, da Comissão Pedagógica e da Comissão de Faina do Curso Mestrado Integrado em Engenharia Electrónica e Telecomunicações dos anos lectivos 08/09 e 09/10 por todos os momentos de trabalho, entreajuda e diversão que me fizeram crescer enquanto pessoa.

A todos os meus amigos pelo acompanhamento e apoio constantes, por todas as noites de sono perdidas a estudar e por todos os momentos de alegria que me proporcionaram.

Aos meus colegas de casa destes meus anos passados em Aveiro, Ângelo Almeida, Miguel Martins, e João Cardoso, e à minha namorada Andreia Pacheco, a eles um muito obrigado pela sua paciência, compreensão e encorajamento.

 Por fim, quero agradecer a toda a minha família, em particular aos meus pais, irmão, e avó pela confiança depositada nas minhas capacidades ao longo da vida.

palavras-chave

resumo

Este trabalho focou-se no estudo dos efeitos cruzados em sistemas de comunicação ópticos passivos. Para isso foram abordados de uma forma genérica os factores cruzados mais relevantes que ocorrem em fibras comuns. Estes foram analisados na perspectiva das aplicações que temos em mãos, que correspondem a redes de acesso baseadas em G-PON e com convivência de canais de vídeo. A característica dos sinais, especificamente a potência do sinal de vídeo evidencia-se como a mais potencial causa de efeitos cruzados, dados os níveis elevados de potência que podem ser transmitidos. Ainda, os efeitos cruzados que parecem os mais relevantes, dada a sua característica de largura de banda elevada, são o Raman e a modulação de fase cruzada e como tal vão ser descritos com mais profundidade. Os resultados apresentados tentam sempre mostrar os efeitos em ambos os sinais e tentam-se obter os resultados para diversos cenários possíveis, os quais, sempre que possível, respeitam as normas respectivas relativas a esses sinais. Em alguns casos, e para demonstrar a validade do processo, são expandidos em termos dos vectores passíveis de controlo mais comuns: a potência, o comprimento de onda e o formato de modulação. Com um formato de modulação avançado pretende-se estudar o potencial da introdução deste tipo de sinais no sistema como soluções viáveis para NGPON2.

keywords

abstract

This work aimed at the study of cross effects in passive access optical communication systems. With that purpose the more relevant cross factors that occur in common fibers were approached. These were analyzed in the perspective of the most recent applications, corresponding to the access networks based on G-PON and with coexistence of video channels. The characteristic of the signals, specifically the power of video signals is seen as the most potential cause of cross effects, since the power levels that are allowed to be transmitted can be rather high. Moreover, from the identified cross effects, the ones that seem to be the most relevant, due to their high bandwidth characteristics, are the Raman and the Cross Phase Modulation and for that reason they will be described deeper depth. The results presented always show the effects in both sources and the targeted results try to observe a variety of possible scenarios, which whenever as possible, respect the related standards. However, for a broader vision, in some cases, the vectors that can be commonly controlled: the power, the wavelength, and the modulation format; are expanded. By studying one advanced modulation format for the digital data it is intended to study their potential for NGPON2.

Table of Contents

List of Figures

List of Acronyms

AM	Amplitude Modulation
AM-VSB SCM	Amplitude Modulation Vestigial Sideband Subcarrier-Multiplexed
APON	Asynchronous Passive Optical Network
ASK	Amplitude Shift Keying
BER	Bit Error Rate
BPSK	Binary Phase Shift Keying
CATV	Cable Television
CNR	Carrier to Noise Ratio
CO	Central Office
CSRZ-OOK	Carrier-Suppressed Return-to-Zero On-Off-Keying
CW	Continuous Wave
DCF	Dispersion Compensating Fiber
DPSK	Differential Phase Shift Keying
DQPSK	Differential Quadrature Phase Shift Keying
DSF	Dispersion Shifted Fibre
EDFA	Erbium Doped Fibre Amplifier
FSK	Frequency Shift Keying
FTTH	Fibre-To-The-Home
FWM	Four-Wave-Mixing
GPON	Gigabit Passive Optical Network
HD-TV	High Definition Television
IM	Intensity Modulation
LD	Laser Diode
MOD	Modulator

MZM	Mach Zehnder Modulator
NGPON	New Generation Passive Optical Network
NRZ	Non-Return-to-Zero
NRZ-DPSK	Non-Return-to-Zero Differential Phase Shift Keying
NRZ-OOK	Non-Return-to-Zero-On-Off-Keying
NTSC	National Television System Committee
OOK	On-Off-Keying
OSNR	Optical Signal-to-Noise Ratio
PON	Passive Optical Network
PSK	Phase Shift Keying
QPSK	Quadrature Phase Shift Keying
RF	Radio Frequency
RIN	Relative Intensity Noise
RZ	Return-to-Zero
RZ-DPSK	Return-to-Zero Differential Phase Shift Keying
RZ-OOK	Return-to-Zero-On-Off-Keying
SPM	Self Phase Modulation
SRS	Stimulated Raman Scattering
SSB	Single Sideband
VSB	Vestigial Sideband
WDM	Wavelength Division Multiplexer
XPM	Cross Phase Modulation

"The greater the difficulty, the greater the glory"

Marcus Tullius Cicero

x

Chapter 1. Introduction

1.1. Context

Even since the beginning of times, human kind has shown a need to communicate and pass information from one place to another. Communication systems had evolved along the times in order to better accomplish the task. That was enabled through the increase the data rate, to the improvement of the transmission fidelity.

In 1838 when Samuel F.B. Morse invented the telegraph, the communications entered in a new era, the electrical communications era. The first commercial telegraph using wire cables was implemented in 1844 and it was spread through the world in the following years. Wire cable was the only medium for electrical communication until Heinrich Hertz discover the long-wavelength electromagnetic radiation in 1887. The first implementation of this was the radio demonstration by Guglielmo Marconi in 1895.

In Electrical Systems, data is usually transferred over the communication channel by superimposing the information signal onto a sinusoidal varying electromagnetic wave which is known as carrier. The amount of information that can be transmitted is directly related with the frequency range over which the carrier wave operates, increasing the carrier frequency the available transmission bandwidth will be increased also.

With the advent of the laser in 1960, great interest in communicating at optical frequencies was created. With optical frequencies on the order of 5e14 Hz, laser has a theoretical information capacity which is approximately equal to 10 million TV channels.

For transmission at optical region two classes of transmission media can be used: an atmospheric channel or a guided-wave channel. In 60s a number of experiments using atmospheric optical channels were made, but its high costs of developing all the necessary components and installation, the limitations of the atmospheric channel imposed by rain, fog, snow, and dust make this communication system economically unattractive. At the same time, investigations into optical fibers were made. The extremely large losses (more than 1000dB/km) observed in the first optical fibers, was proved to be caused by the impurities in the fiber when in 1970, Kapron, Kleck, and Maurer fabricated a silica fiber having a 20dB/km attenuation. At this attenuation, repeaters spacing for optical fiber links become comparable to those of cooper systems.

The combination with the semiconductor technology, which provided the necessary light sources and photodetectors, enhanced the development of optical fiber systems growth. These systems had some inherent advantages over conventional copper systems, such as: low transmission loss and wide bandwidth, small size and weight, immunity to electromagnetic interference, electrical isolation, signal security and abundance in raw material.

Since the moment where the fiber losses were reduced to a low level, in 1970, in less than two decades, more than 10 million kilometers of fiber had been installed all over the world. The first links in 1977 operated at 800nm using GaAs-based optical sources, silicon photodetectors, and multimode fibers. A change from 800nm to 1300nm in the operation wavelength and from multimode to single mode fibers occurred in 1984 allowing to increase repeaterless transmission distance, the bandwidth, and to reduce the losses. Links at 1550nm were the next evolutionary step. These systems provide the lowest attenuation, but have much larger dispersion than the 1300nm links. Since the dispersion can be controlled by recurring to special fibers like DSF and DCF, links at 1550nm attracted much attention for high-capacity and long-haul links. With these evolutions and with the advent of the optical amplifiers was possible to increase even more the transmission distance and the bandwidth of the optical fiber systems.

With the evolution of the optical systems, optical transmission standards have also evolved significantly, and nowadays Passive Optical Networks (PONs) assume an important role in optical communications. A PON is a point-to-multipoint fiber network in which optical splitters are used to enable a single fiber to serve multiple clients and takes advantage of wavelength division multiplexing (WDM), using one wavelength for downstream traffic and another for upstream on a single fiber.

One of PON standards is GPON (Gigabit PON) [1], this standard uses 1490nm wavelength and typically a bit rate of 2.488Gb/s for downstream traffic, 1310nm wavelength and 1.244Gb/s for upstream traffic and 1555nm for video overlay. The work presented in this dissertation intends to study the cross effects that appears from the video and data transmission in the downstream path.

1.2. Motivation

GPON is being commercialized in several countries in the world. In some of them the penetration is already very high, like North Korea, Sweden, Japan, and United Arab Emirates. In Portugal, the government in cooperation with several operators is promoting the expansion of this technology through all the territory, making possible the access to a large portion of the population. The bandwidth provided by GPON equipments will be enough to the most part of the urban cases, however, the appearance of new services like HD-TV or WEB 2.0 will require in a near future, an increased the network performance.

When PON is deployed with the 1555nm [2] wavelength for video overlay, one of the issues that the operator may encounters is related to the non-linear effects. The video signal is transferred with much higher power than the data signal, and this could lead to the appearance of some cross effects that will affect the performance of data signal. To this configuration two signals are transmitted through the same fiber in downstream path. The signals may interact with each other in a non-linear way and, undesired effects will appear such as cross-phase modulation, stimulated Raman scattering, and four-wave-mixing.

These undesired effects will cause degradation in the signals being responsible by some degradation in the system performance.

With the need of increase bandwidth and performance of the systems in the actual scenario, these effects cannot be ignored and its study becomes fundamental to the definition of the parameters and choice of the components.

1.3. Structure and Objectives

This document is divided in five chapters, and the final objective is to study the cross effects between the data and the video channels in some scenarios, one of them the PON scenario.

In this first chapter the context of this work is presented with the motivation, main proposed objectives and the structure of the studies.

The second chapter describes the main nonlinear effects in optical fibers, and a survey on methods to minimize their effects in the system performance.

In the third chapter we present a brief description of the most usual modulation formats, like the intensity modulated, coherent and differential signals. In this chapter the video overlay signal is also presented in terms of its modulation format and how it is affected by non-linear effects like Stimulated Raman Scattering.

In chapter 4, by means of simulation, the simultaneous transmissions of video and data signals are studied. The video signal is composed by NTSC channels transmitted in the video distribution band (according to G.983.3). For the data, some parameters will be changed, like the modulation format used, the power of the channel, the channel separation between video and data, the transmission band. To evaluate the video channel, Carrier-to-noise (CNR) measurements will be used. To evaluate data, the Bit-Error-Rate (BER) will be estimated.

In the final chapter, the conclusions drawn from the work presented in this dissertation and suggestions for future work will be made.

1.4. Main Contributions

In the author's opinion, the main contributions of this work may be summarized as follows:

- Identification of the main sources of X-talk in PONs

- Given the existing standards, the main potential x-talk signals were identified

- The X-talk between video and data channels was studied

- The limitations in propagation for video and data signals when sharing in the same PON were identified and quantified.

- One advanced modulation format, potential for NGPON2, was studied and its impact on and from the video channel characterized by means of simulation.

Chapter 2. Non-Linear Effects

2.1. Introduction

Non-linear effects have an important role in the propagation of the signals in optical fibers. Neglecting them or not efficiently compensating them can lead to uncontrolled signal degradation, which can result in increasing the BER and make difficult reception of data. In this chapter some of the non-linear effects will be exposed, they are: Cross-Phase Modulation (XPM); Self-Phase Modulation (SPM); Four-Wave-Mixing (FWM) and Stimulated Raman Scattering (SRS).

2.2. Self-Phase Modulation (SPM)

The Self-Phase Modulation is related with the change of phase in the electromagnetic field in a fiber caused by its own amplitude and by the fiber refraction coefficient. This phenomenon can be explained better looking at the expression that determines the evolution of electromagnetic field along a fiber [3]:

$$\phi = nk_0L$$

(2.2.1)

And to the expression of refraction index:

$$\tilde{n}(\omega, |E|^2) = n(\omega) + n_2|E|^2 \qquad (2.2.2)$$

This index includes a non-linear component that cannot be ignored. Using the expression of (2.2.1) in (2.2.2), (2.2.3) can be obtained, which represents the phase variation with the propagating field:

$$\phi = \tilde{n}k_0L = (n + n_2|E|^2)k_0L$$

$$(2.2.3)$$

In (2.2.3) is possible to identify the non-linear phase component of the stemming from the refraction index, is given by:

$$\phi_{NL} = n_2|E|^2k_0L \qquad (2.2.4)$$

Where,

$$k_0 = 2\pi/\lambda \qquad (2.2.5)$$

As a result of this change of phase, new frequencies in the electromagnetic field will appear, causing spectrum enlargement. In the figure 2.2.1 can be seen the shift in the frequency caused by one Gaussian pulse. The front of the pulse will suffer a negative chirp causing a decrease on its frequencies while the back of the pulse will suffer a positive chirp causing an increase on its frequencies.

The effect caused by this chirp will depend on the dispersion regime of the wavelength range where the pulse propagates. If the dispersion regime is normal, $\beta > 0$, the higher frequencies tend to travel slowly and the lower frequencies tend to travel faster, causing enlargement of the pulse. If the dispersion regime isn't normal, $\beta < 0$, the opposite is verified and a compression of the pulse occurs.
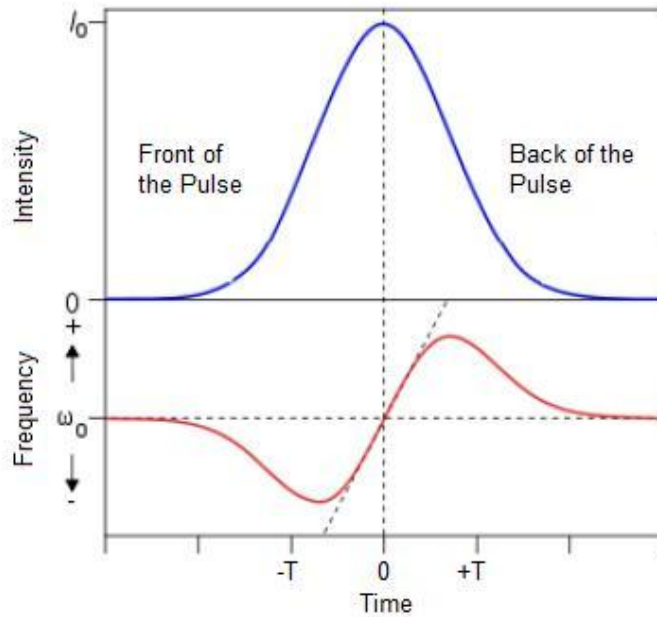
Figure 2.2.1 – Temporal variation of frequency shift caused by SPM in a Gaussian Pulse

2.3. Cross-Phase Modulation (XPM)

If two or more signals travels through the fiber at the same time, they will interact leading to non-linear effects such has Cross-Phase Modulation (XPM) or Four-Wave-Mixing (FWM).

Cross-Phase Modulation (XPM) is always accompanied by self-phase modulation (SPM) because both occur due to the dependence of the refractive index with the intensity of electromagnetic field in the fiber. XPM occurs because the effective refractive index seen by an optical beam in a nonlinear medium depends not only on the intensity of that beam but also on the intensity of other co-propagating beams with different wavelength, direction and/or polarization.

For better understanding of this phenomenon, the simultaneous co-propagation of two signals with polarization along the *xx* axis is considered, and the resulting electromagnetic field is given by the expression (2.3.1) [3]:

$$E = \frac{1}{2}\hat{x}[E_1 exp(-i\omega_1 t) + E_2 exp(-i\omega_2 t) + c.c.]$$

(2.3.1)

Where *c.c.* means complex conjugate.

The nonlinear phase shift can be written as in (2.3.1)

$$\phi = n_2 k_0 L(|E_1|^2 + 2|E_2|^2)$$

(2.3.2)

The first term of the expression (2.3.2) is due to the self-phase modulation and the second term is due to the cross-phase modulation. In that expression can be seen also that when two signals with equal intensity and polarization travel through the fiber, XPM effect is twice more strong that the effect of SPM.

XPM as SPM leads to enlargement of the spectrum, but such enlargement can be asymmetric. If the signals co-propagating in the fiber have not the same power, looking at the expression (2.3.2) is easy to understand that the XPM effect will not be noted in both the signals in the same way.

To get some insight in the behaviour of XPM effect a simulation using the VPI Systems software was made [4]. The setup in study was the following:
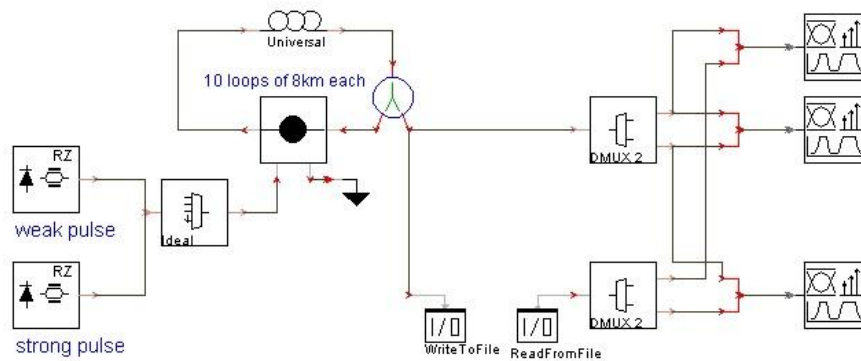
Figure 2.3.1 – VPI Systems setup to study XPM effect

In this setup, one weak pulse (2mW of peak power) and one strong pulse (20mW of peak power) will be transmitted. These two pulses will be multiplexed and then pass through 10 loops of 8 km each. In the fibre output a demux is inserted to separate the

pulses, and these pulses will be analyzed separately by signal analyzers. In a first step the XPM and the SPM parameters are turned off in the fibre, and the results will be saved in a file. In a second step, these parameters are enabled and the results previously saved will pass through a demux to separate the pulses and then analyzed together with the new results in the signal analyzers.

In the simulation, a pulse walks through another pulse in a different WDM channel interacting because both affect the refractive index of the fibre, as described. The optical spectrum of the weak pulse before and after the collision will be shown in the next figure:
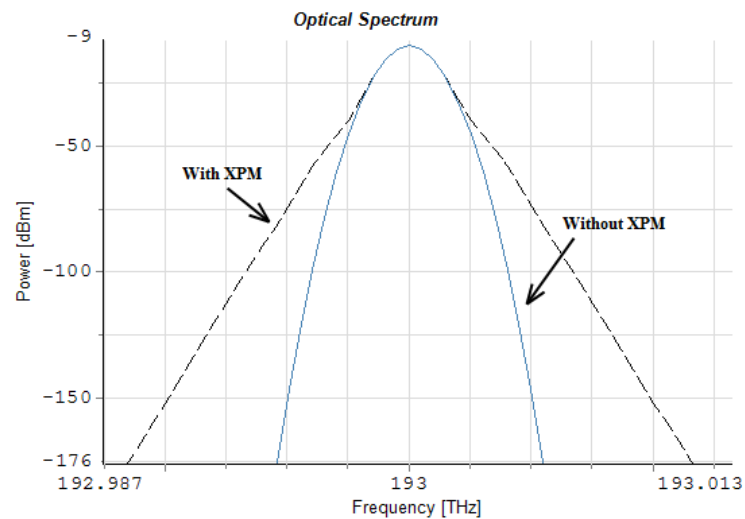
Figure 2.3.2 – Optical Spectrum of the weak pulse with (black and dashed) and without (blue and solid) XPM effect

As the strong pulse is 10 times stronger than the weak signal, its effect will be noted clearly in the weak signal because of the XPM effect. In figure 2.3.2 can be seen that the presence of XPM causes broadening on the weaker signal.

2.4. Four-Wave Mixing (FWM)

The four-wave-mixing is a phenomenon that stems from the nonlinear response of bound electrons of a material to an applied optical field. More specifically, the polarization induced in the medium is non linear in the applied field but contains nonlinear terms whose magnitude is governed by the nonlinear susceptibilities.

The polarization term can be given as [3] :

$$P = \varepsilon_0 \left(\chi^{(1)}.E + \chi^{(2)}:EE + \chi^{(3)}:EEE + \cdots \right)$$

(2.4.1)

From (2.4.1) the term in more focus must be the 3rd order susceptibility that is responsible for the four-wave-mixing, and so can be written:

$$P_{NL} = \chi^{(3)}:EEE$$

(2.4.2)

Consider four waves oscillating at frequencies ω_1, ω_2, ω_3, ω_4 and linearly polarized along the same axis x. The total electric field can be written as:

$$\mathbf{E} = \frac{1}{2}\hat{x}\sum_{j=1}^{4} E_j \exp[i(k_j z - \omega_j t)] + \text{c.c.}$$

(2.4.3)

With:

$$k_j = n_j \omega_j /c$$

(2.4.4)

The four waves are assumed to propagate in the same direction.

Using the expression (2.4.3) in (2.4.2) comes:

$$P_{NL} = \frac{1}{2}\hat{x}\sum_{j=1}^{4} P_j \exp[i(k_j z - \omega_j t)] + c.c$$

(2.4.5)

And can be found that Pj (j= 1 to 4) consists of a large number of terms involving the products of three electric fields. P_4 can be expressed as:

$$P_4 = \frac{3\varepsilon_0}{4}\chi_{xxxx}^{(3)} \left[|E_4|^2 E_4 + 2(|E_1|^2 + |E_2|^2 + |E_3|^2)E_4 \right.$$
$$\left. + 2E_1 E_2 E_3 \, exp(i\theta_+) + 2E_1 E_2 E_3^* \, exp(i\theta_-) + \cdots \right] \qquad (2.4.6)$$

Where θ_+ and θ_- are defined as:

$$\theta_+ = (k_1 + k_2 + k_3 - k_4)z - (\omega_1 + \omega_2 + \omega_3 - \omega_4)t \qquad (2.4.7)$$

$$\theta_- = (k_1 + k_2 - k_3 - k_4)z - (\omega_1 + \omega_2 - \omega_3 - \omega_4)t \qquad (2.4.8)$$

The first four terms containing E_4 in the expression (2.4.6) are responsible for the SPM and XPM effects. The remaining terms result from FWM. Significant FWM occurs only if phase mismatch is almost null.

In the expression (2.4.6) the term containing θ_+ corresponds to the case in which three photons transfers their energy to a single photon at frequency $\omega_4 = \omega_1 + \omega_2 + \omega_3$. The term containing θ_- in the same expression correspond to the case in which two photons at frequencies ω_1 and ω_2 are annihilated with simultaneous creation of two photons at frequencies ω_3 and ω_4 such that:

$$\omega_3 + \omega_4 = \omega_1 + \omega_2 \qquad (2.4.9)$$

The phase matching requirement for this process to occur is:

$$\Delta k = k_3 + k_4 - k_1 - k_2$$
$$= (n_3\omega_3 + n_4\omega_4 - n_1\omega_1 - n_2\omega_2)/c = 0 \qquad (2.4.10)$$

It is relatively easy to satisfy $\Delta k = 0$ in the specific case $\omega_1 = \omega_2$. This manifests as a strong pump wave at ω_1 that creates two sidebands located symmetrically at frequencies ω_3 and ω_4 with a frequency shift given by:

$$\Omega_s = \omega_1 - \omega_3 = \omega_4 - \omega_1 \qquad (2.4.11)$$

Where is assumed that $\omega_4 > \omega_3$.

The number of FWM products generated by N waves is given by [5] [23]:

$$M = \frac{1}{2}(N^3 - N^2)$$

<div align="right">(2.4.12)</div>

In the figure 2.2.3.1 can be seen the FWM products generated in the case of four waves propagating in the fibre. Following the expression (2.4.12), these four-waves lead to the appearance of M = ½ (4³ - 4²) = 24pulses.
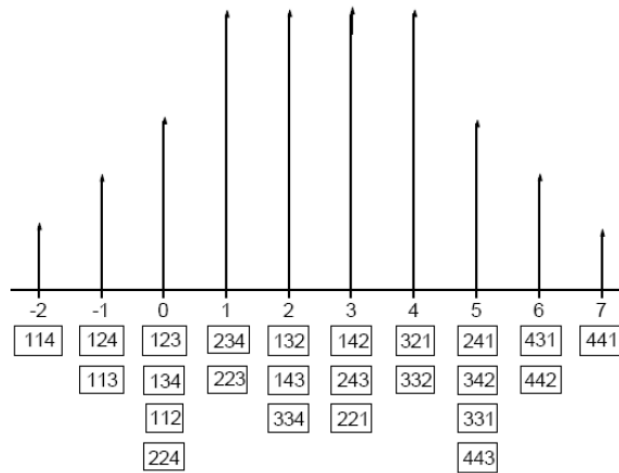
Figure 2.4.1 – Pulses generated by FWM

2.4.1 Techniques to reduce FWM crosstalk

The attractiveness of light wave communications is the ability of silica-optical fibres to carry large amounts of information over long distances. To utilize the available bandwidth, numerous channels at different wavelengths can be multiplexed on the same fibre (WDM systems) [6]. In such all-optical systems the effects of chromatic dispersion and nonlinearities accumulate during light propagation, imposing limits on the achievable performance. The use of dispersion-shifted fibres (DSF) can reduce the chromatic dispersion at 1550nm, but its use will enhance the efficiency of four-wave mixing products generation, reducing the phase mismatch that depends of fibre dispersion [7] [8].

Several different techniques to reduce FWM crosstalk have been proposed, but there are some points that we have to look at when we chose the method to use: the method

chosen must be cost effective, accurate, easy to apply, and robust enough to account for a large number of constraints, such as total allowable power and channel spacing [9].

FWM efficiency depends on phase mismatch, which depends on channel separation and fibre dispersion coefficient [10], and so the next studies are focused on this.

First, a reduction of FWM crosstalk based on fibre dispersion coefficient is going be made, and then a reduction based on a system with unequal spaced channels.

2.4.1.1 Reduction of FWM crosstalk by changing the fiber dispersion coefficient and by elimination of one of the channels

To study this technique, some simulation was made, using the next setup based on VPI Systems software:

Figure 2.4.1.1 – VPI Systems Setup: 4 x10 Gbit/s WDM transmission over Dispersion Shifted Fiber (DSF)

In this setup, four NRZ signals with equal average power are multiplexed and then transmitted through 50 loops of a DSF fibre with 1 km of length and 0.2 dB/km of attenuation. A signal analyzer is used to observe the output optical spectrum. The fibre

output passes through a demux 1x8, being its outputs used to observe the eye diagrams of the NRZ signals and the FWM products.

In the above simulation, two cases were studied, first to the case of a low dispersion fibre of D=0.2ps/nm/km and then increasing the dispersion of the fibre to D=2.0ps/nm/km. To both cases another two schemes were analysed:

- Four pulses propagating;

- Three pulses propagating, turning off channel 2.

In the next two figures can be seen the Optical Spectrums and the eye diagrams to the case of D = 0.2ps/nm/km:

Figure 2.4.1.2 – Output optical spectrums: In the left side the case of four-wave propagation is showed and in the right side the case of channel 2 turned off can be seen.
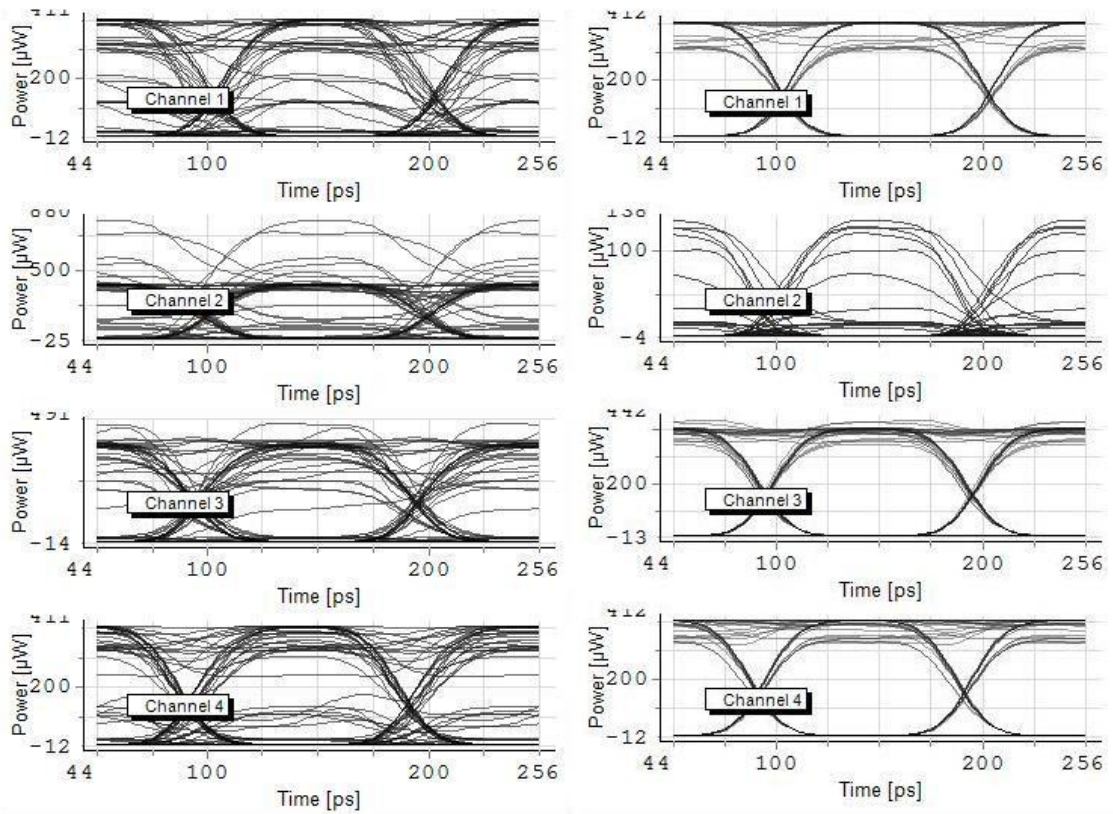
Figure 2.4.1.3 – Eye diagrams: in the left side is the case of four-wave propagation; in the right side is the case of channel 2 turned off.

Case of four pulses propagating:

In the figure 2.4.1.2 at the left side the emergence of the FWM products is clearly seen and the approximation between the optical power of these products and the data channels is verified. In the eye diagrams, in this case (figure 2.4.1.3 – left side) can be seen the presence of some distortion caused by the crosstalk. Some FWM products will appear in the same wavelength than the signal pulses causing signal degradation affecting the eye diagrams.

Case of propagation with channel 2 turned off:

In this case, the effect of the channels 1, 3 and 4 on the channel 2 wavelength can be observed in the output optical spectrum with the appearance of a FWM product at this wavelength. The eye diagrams of the three channels propagated are cleaner and that

can be explained by the absence of the channel two, that did not influence the other channels now reducing the number of FWM products generated. The different separation of the signals can also be helpful to the lower signal degradation by shifting the FWM products from the wavelengths of the signals to out of there [7] [8] [11]. The performance increase of the system in this case can be also observed by looking at the power of the FWM products created. The power of these channels are low now than in the previous case.
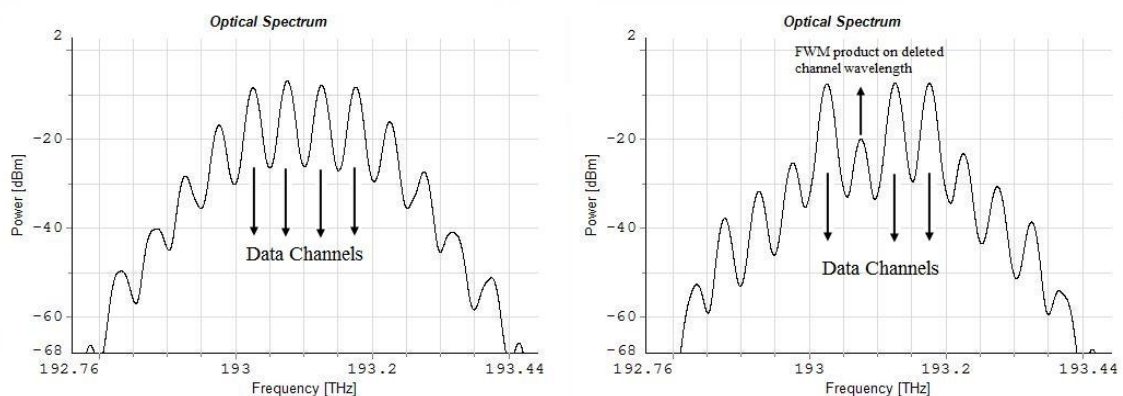
Case of D = 2.0ps/nm/km:
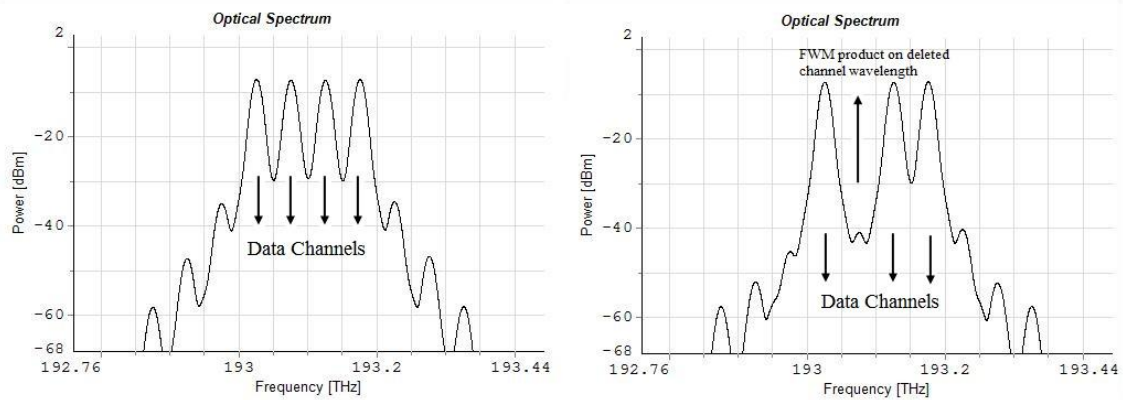
Figure 2.4.1.4 – Optical Spectrums: : In the left side the case of four-wave propagation is showed and in the right side the case of channel 2 turned off can be seen.
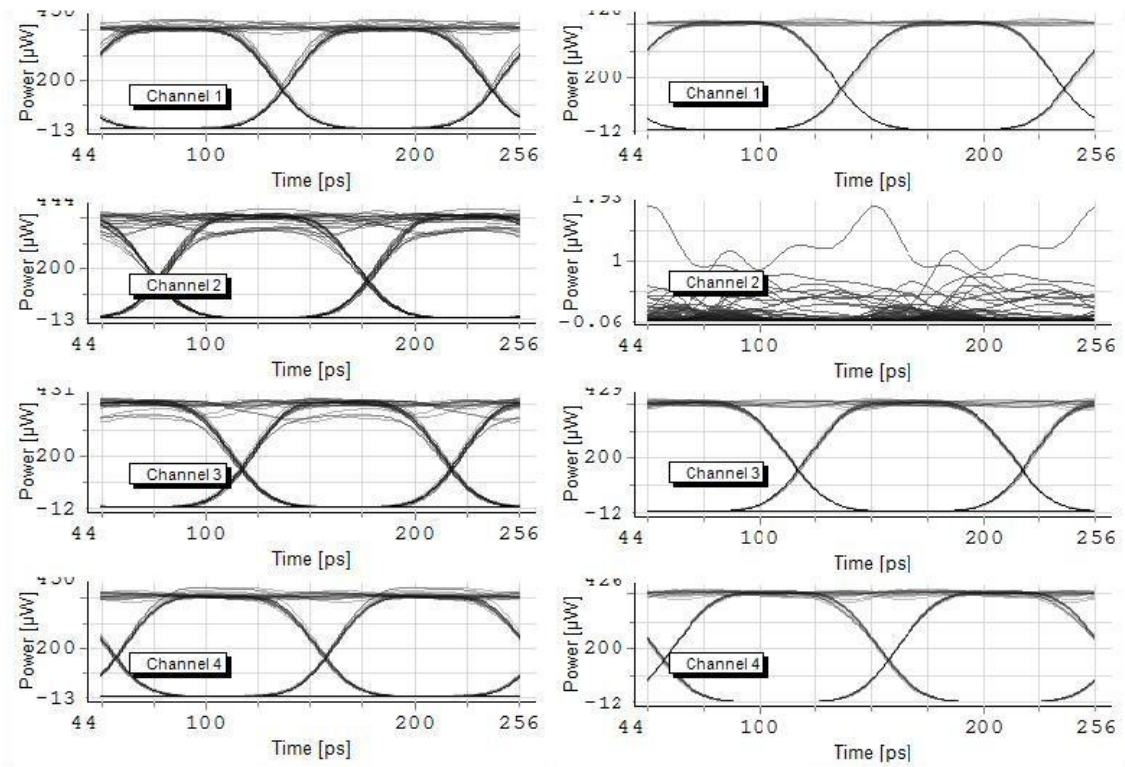
Figure 2.4.1.5– Eye diagrams: left side) the case of four-wave propagation; right side) the case of channel 2 turned off.

From the above figures can be seen that in the case of D = 2.0ps/nm/km the effect of FWM is lower than in the case of the 0.2ps/nm/km. In this case, in the optical spectrum can be seen a lower optical power of FWM products compared with the case of lower dispersion in the fibre. In the eye diagrams of figure 2.4.1.5 lower noise can be observed also. That could be explained locking at the expression of FWM signal power that is given by:

$$P_{FWM} = \frac{\eta}{9} d^2 \gamma^2 P_0^3 \exp(-\alpha L) \cdot L_{eff}^2$$

(2.4.1.1)

Where η is the efficiency of the mixing that is given by the expression (2.4.1.2):

$$\eta = \frac{\alpha^2}{\alpha^2 + \Delta\beta^2} \left(1 + \frac{4e^{-\alpha L} \sin^2(\Delta\beta L / 2)}{(1 - e^{-\alpha L})^2} \right)$$

(2.4.1.2)

The efficiency depends on the dispersion through Δβ as the next expression shows:

$$\Delta\beta = \frac{2\pi\lambda^2}{c} D \cdot \Delta f^2$$

(2.4.1.3)

From the above expression can be seen that the dispersion and the channel spacing are the higher contributors to the FWM products appearance. So, if the dispersion is small, Δβ≈0, so η≈1 and the FWM can have a huge impact in the performance of the system. In Figure 2.4.1.6 the FWM signal power evolution with the fibre length and the channel spacing can be observed:
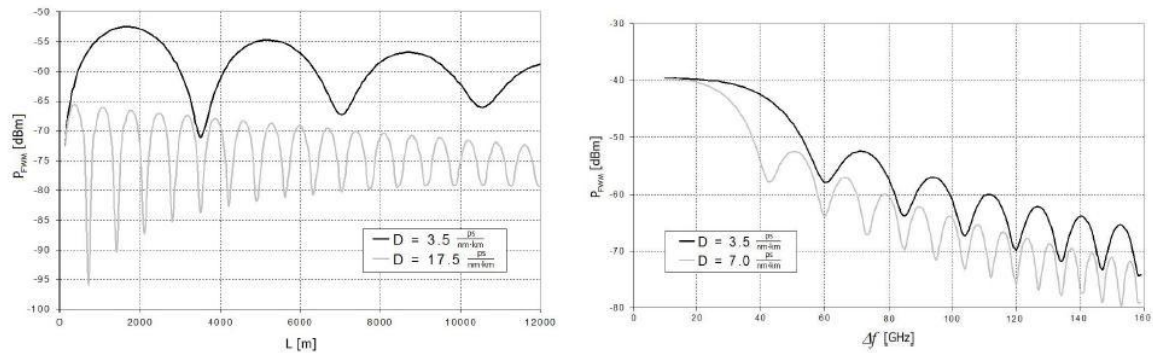
Figure 2.4.1.6 – FWM signal power in function of fibre length and channel spacing for different values of dispersion [10]

2.4.1.2 Reduction of FWM crosstalk using unequal channel spacing

To reduce FWM crosstalk in WDM systems, a technique based on unequal-spaced channel allocation can be used. The use of this technique has the main objective of prevent the FWM products from fall at the channel frequencies. If the frequency separation of any two channels of a WDM system is different from that of any other pair of channels, no FWM waves will be generated at any of the channels, thereby suppressing FWM crosstalk [7],[8]. Although the unequal-spaced channel allocation techniques greatly reduce FWM crosstalk, the number of unequal-spaced WDM channels supported is always

less than that of conventional equal-spaced WDM systems when the operating optical bandwidth and the minimum channels spacing of both kinds of systems are the same [12].

To a better understanding of this technique a study was made, using the simulation setup of Figure 2.4.1.7:
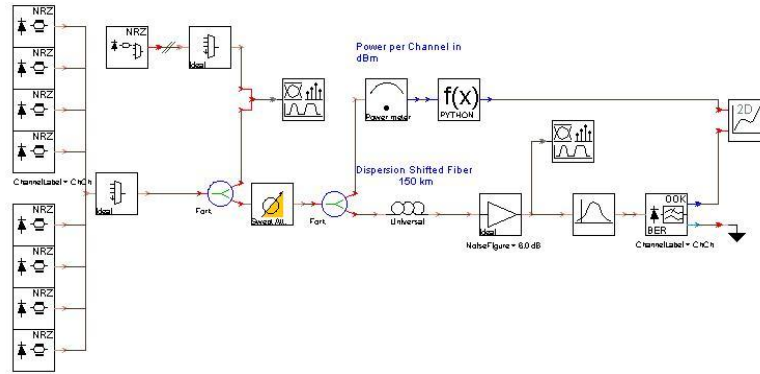
Figure 2.4.1.7 – Setup to study the reduction of FWM effect using unequal channel spacing

In the above system 8 NRZ signals will be transmitted with equal and unequal channel spacing. These signals will be multiplexed and then pass through a swept attenuator. An increasing attenuation is applied to each block, being useful for producing BER versus Received Optical Power plots. The output of the swept attenuator will be sent to a DSF fiber of 150km and then amplified. The channel four will be used for BER estimation, filtered before the OOK receiver by an optical filter centered at the required frequency.

In the next figures the channel plans and the results of BER vs. Average Channel Power are shown:

20
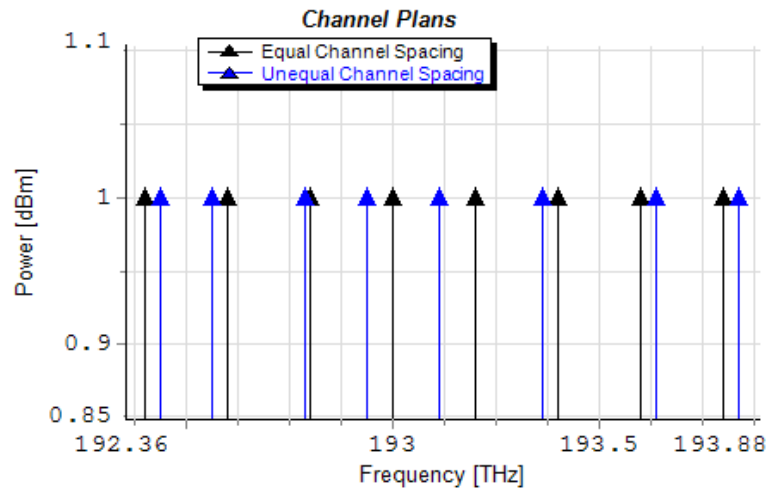
Figure 2.4.1.8 – Channel plans for normal and unequal channel spacing
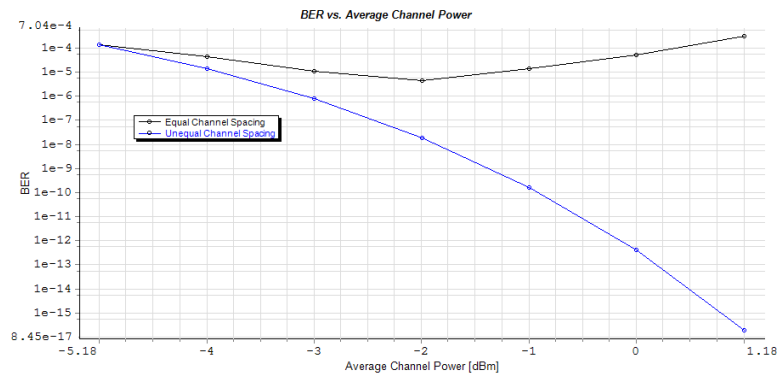
Figure 2.4.1.9 – BER vs. Average Channel Power

In [7] a WDM system with eight channels was studied when these channels are transmitted over 137 km of DSF. And the next figure can be observed to a better understanding of the above results:
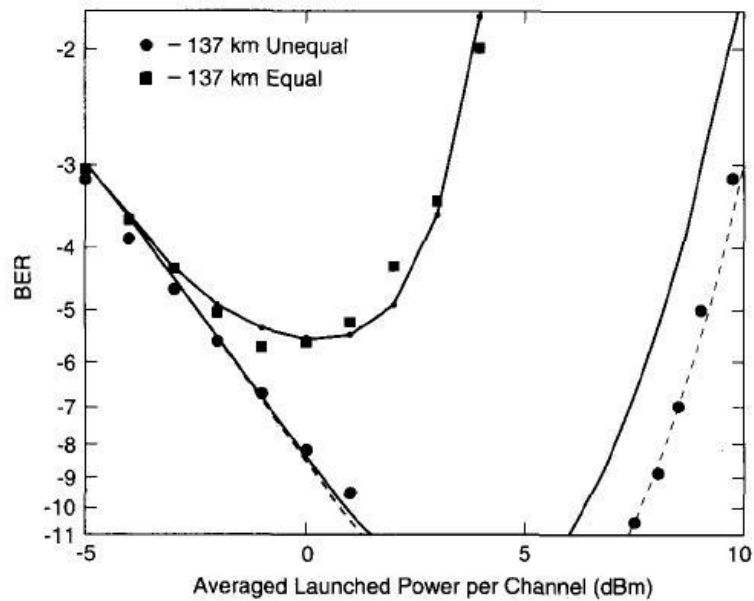
Figure 2.4.1.10 – Probability of error of the third channel versus launched power per channel. The continuous line shows the theoretical result for unequal channel spacing. The dashed line is obtained from the theory with a 30% reduction of efficiency and the small dots connected with a line are the simulation results for equal channel spacing

From Figure 2.4.1.10 it can be seen that the simulation and the expected results are close to each other. For low power levels both wavelength distributions (equal and unequal) have approximated results therefore pointing to the low impact of the FWM. When the launched power increases, the equal spaced channels system is dramatically affected by the FWM and performance is degraded, BER lower than 1E-6 is not achieved. The unequal channel spaced system, however does not suffers from FWM interference. Its BER keeps decreasing. 1E-9 is achieved for -1.5dBm in the figure 2.4.1.9 and for 0dBm in the figure 2.4.1.10 [7]. In figure 2.4.1.9 the increase of BER caused by other nonlinear effects cannot be observed, but in 2.4.1.10 it can. The BER is lower than 1E-9 for values of input power per channel between around 0dBm and +7dBm allowing a wide range of operation.

This technique allows fibre input power to be increased by as much as 7dB over the conventional equal channel allocation system. This allows a decrease on the receiver sensitivity. Alternatively the higher input power allowed by unequal channel spacing can be exploited by increasing system length for the same bit rate that was used in equal channel spacing [7].

Although the FWM crosstalk minimization this technique has the disadvantage of bandwidth expansion, that increases with the number of WDM channels. The total bandwidth required to unequal channel spaced systems is presented in the next expression:

$$B_{un} \geq \left(1 + \frac{\frac{N}{2} - 1}{n}\right) B_{eq}$$

(2.4.1.4)

Where N is the number of channels, and n is the minimum channel separation in number of slots.

In the next table can be analysed the different bandwidth expansion factors to different cases in WDM systems with 4, 8 or 10 channels and chose the channel spacing to achieve a desired expansion:

N	n	Channel Spacings								N_{un}	N_{eq}	B_{un}/B_{eq}
4	1	1	3	2						6	3	2.0
4	2	2	3	4						9	6	1.5
4	5	5	6	7						18	15	1.2
4	10	10	11	12						33	30	1.1
8	1	1	3	5	6	7	10	2		34	7	4.9
8	2	6	9	7	4	8	2	3		39	14	2.8
8	5	7	5	8	9	6	10	11		56	35	1.6
8	10	10	11	12	13	14	15	16		91	70	1.3
10	1	1	5	4	13	3	8	7	12	2	55	9	6.1
10	2	6	2	15	3	10	9	5	7	4	61	18	3.4
10	5	5	10	6	8	9	11	7	12	13	81	45	1.8
10	10	10	11	13	12	14	15	16	17	18	126	90	1.4

Figure 2.4.1.11 – Examples of optimum unequal channel spacing [7]

In the above table *Nun* is the total number of slots for unequal channel spacing, *Neq* is the number of slots for equal channel spacing, and *Bun/Beq* is the bandwidth expansion ratio.

In the table can be seen that to a small number of channels a small n can be chosen and the bandwidth expansion factor will not be highly affected, but for a large number of channels the value of n must be as large as possible to avoid a large bandwidth expansion.

2.5 Stimulated Raman Scattering (SRS)

Stimulated Raman Scattering (SRS) is an important process that can turn optical fibres into optical amplifiers or Raman Lasers. This process can also limit the performance of multichannel systems, transferring the energy from a channel to the neighbour channels.

In any molecular medium, SRS can transfer a part of power from one optical field to another field, whose the frequency is downshifted by an amount determined by the vibrational modes of the medium. Basically, the incident light works as a pump and the incident photon loses its energy creating another photon with lower energy. The excess energy is absorbed by the medium under the form of molecular vibrations.

If in a fibre a signal with frequency ωs and a pump with frequency ωp where ωs < ωp, the energy will be transferred from the pump to the signal along the fibre length. The difference Ω = ωp − ωs is called Stokes translation. The initial increase of the Stokes wave is described by [3]:

$$dI_s/dz = g_R I_p I_s$$

(2.5.1)

The first term of the right side is the Raman coefficient and depends on the composition of the fibre core and can vary significantly with the use of different dopants. On the figure 2.5.1 can be seen the Raman coefficient for silica fibre as a function of frequency shift at a pump wavelength of 1μm.
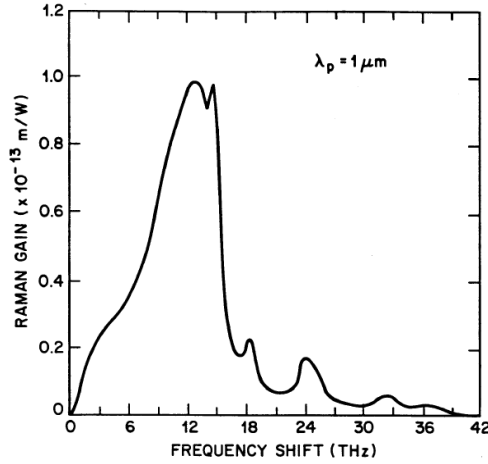
Figure 2.5.1 – Raman-gain spectrum for silica fibers at a pump wavelength of 1μm.

The most important aspect of the Raman gain in optical fibres is that, it extends over a large band of frequencies (close to 40THz) with a peak located close to 13THz. This behaviour is due to the noncrystalline nature of silica glass, and so the fibres can work as large band amplifiers.

The factor of the optical gain is proportional to the intensity of the pump, as the next expression shows:

$$g(\omega){=}g_R(\omega)I_p{=}g_R(\omega)P_p/a_p \tag{2.5.2}$$

In a fiber with length L, the gain obtain is given by expression (2.5.3):

$$G(\omega){=}exp[g(\omega)L] \tag{2.5.3}$$

The Raman threshold is defined as the input pump power at which the Stokes power becomes equal to the output pump power:

$$P_s(L) = P_p(L) \equiv P_0 \exp(-\alpha_p L) \tag{2.5.4}$$

To a better understanding of Stimulated Raman Scattering (SRS) some simulations using VPI Systems software were made. Firstly, the objective was to observe the Raman threshold, and to achieve that, two cases were studied. The case of a pump

wave with higher power than the Stokes wave was first studied, and next the case of pump and Stokes wave with the same power. The setup used is shown in the figure 2.5.2:
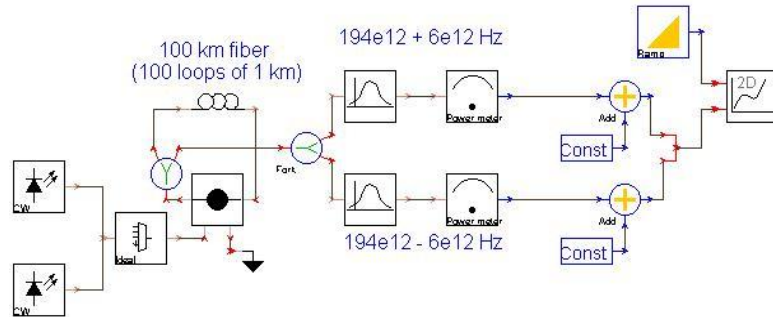
Figure 2.5.2 – Setup to study the SRS

In the above setup, two continuous waves separated by 12THz are multiplexed and transmitted along 100 loops of 1km fibre. The signals are then filtered and the power levels of each signal will be measured and compared.

In the next figure is shown the case in which, pump power is 1W and Stokes power is 1mW:
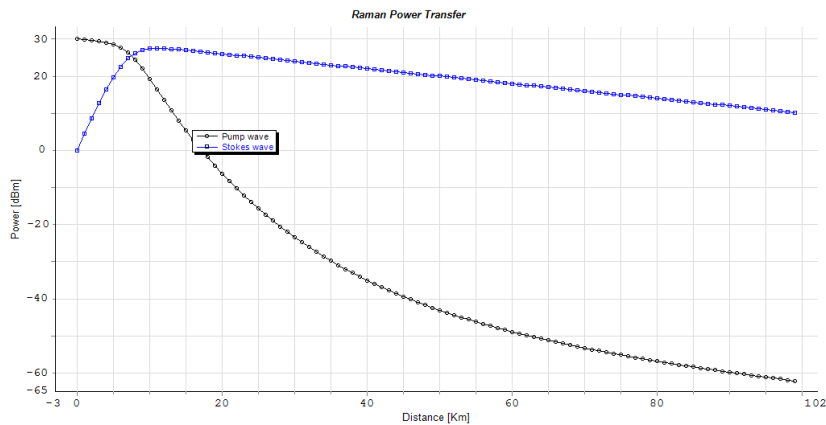
Figure 2.5.3 – Raman power transfer to the case of pump power higher than Stokes power

In next figure is shown the case in which pump power is 1mW and Stokes power is 1mW:
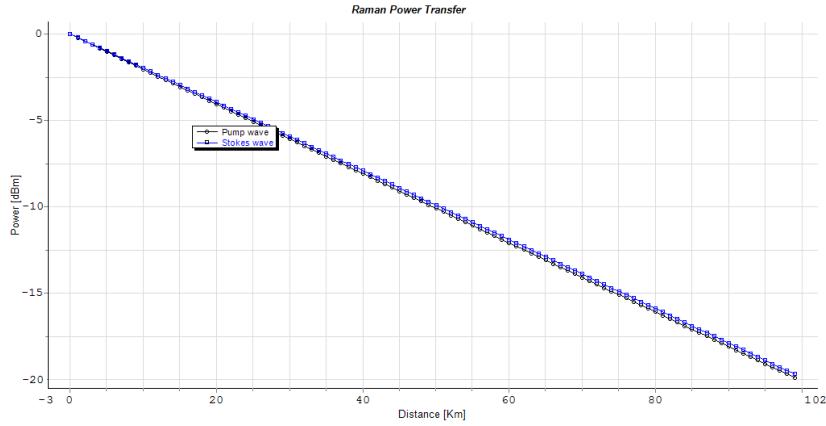
Figure 2.5.4 – Raman power transfer in the case where the pump power equals signal power

In Raman process, the stimulation occurs when the pump power exceeds a certain power level known as threshold power [12]. The threshold condition can be approximated by:

$$P_{th} \approx \frac{16A_{eff}}{g_R L_{eff}}$$

(2.5.5)

With *Aeff* being the effective area of the fibre, the *gR* the Raman gain, and *Leff* the effective length that can be written as:

$$L_{eff} = \frac{1 - \exp(-\alpha L)}{\alpha}$$

(2.5.6)

In the above system, *Aeff* = 80e-12 and *Leff* = 21.48km. The channel separation is 12THz and so from figure 2.5.1 the Raman gain as a value of about 0.8e-13 m/W. From this values, a threshold power of about *Pth* = 745mW.

In that system, the first case studied with pump power of 1W the threshold power is achieved and so the Raman scattering is present that can be seen in the figure 2.5.3. In the case of pump power equal to stokes power at 1mW the threshold is not achieved and so, no Raman scattering is present causing almost no power transfer between the pump and the stokes waves.

In optical communication systems the channel powers are typically below 10mW and so SRS in not a limiting factor for single-channel lightwave systems. However it can affect the performance of WDM systems considerably [12]. In WDM systems numerous wavelengths are injected in to the fibre and the signals at longer wavelengths will be amplified by the shorter wavelength signals. This will lead to system degradation at lower powers than in the single-channel case [6].

In the second simulation using VPI Systems software, a system with 100 channels was simulated. All the channels have the same input power of 1mW. These channels are multiplexed and transmitted along a 50km DSF and then amplified. The effect of higher frequency channels in the lower frequency channels will be analyzed comparing the power of the channels and the eye diagrams of channels 1, 50, 51 and 100. The setup can be seen in the figure 2.5.5.
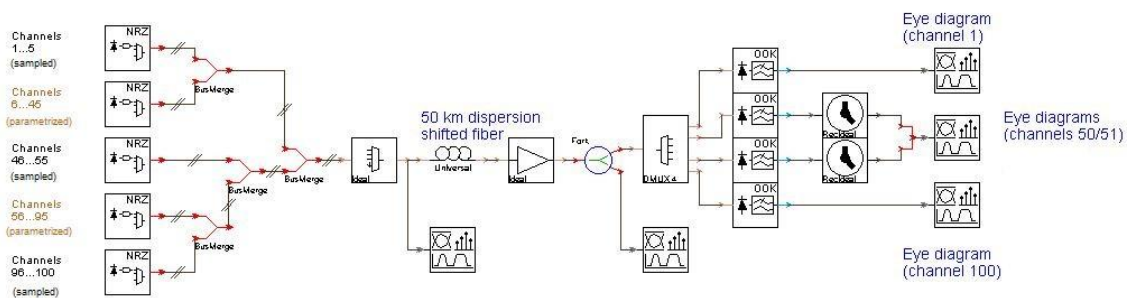
Figure 2.5.5 – Setup to study Raman Effect in a 100 channels system

The optical spectrums at input and output links is shown in figures 2.5.6 and 2.5.7:
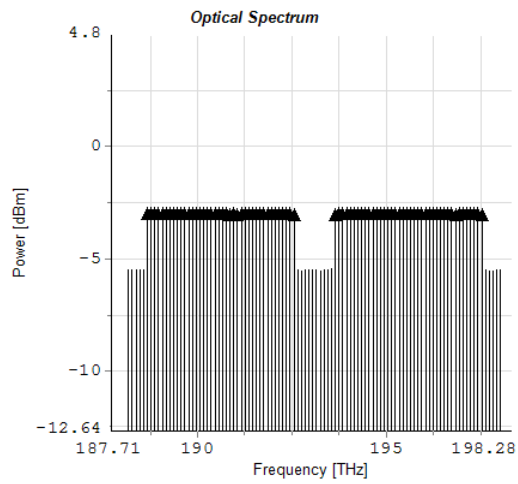
Figure 2.5.6 – Optical Spectrum at input of the link
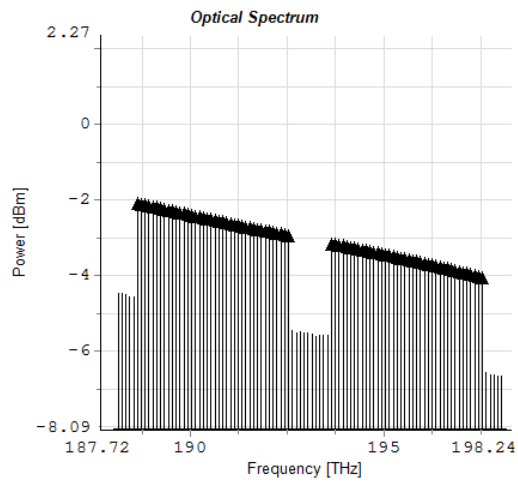
Figure 2.5.7 – Optical Spectrum at output of the link

In the next figure the eye diagrams of channel 1, 50, 51 and 100 are shown:
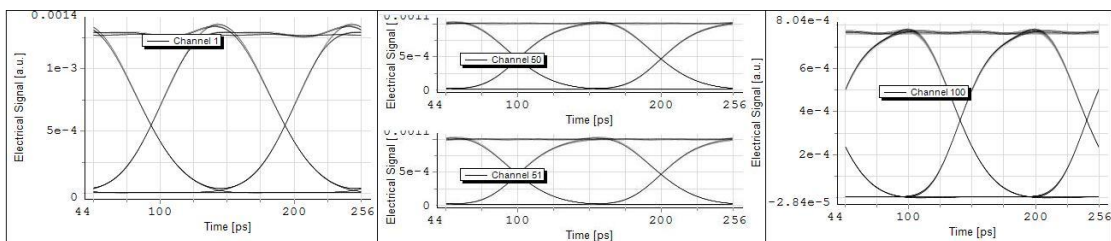
Figure 2.5.8 – Eye diagrams: In the left side channel 1; in the middle 50 and 51 channels; in the right side channel 100

From the eye diagrams is possible to see that the channel 100 shows a more closed eye diagram than the remaining. In this system is possible to notice the appearance of SRS effect, which makes the higher frequency channels work as pump to the lower frequency channels transferring some of its energy to that channels. The channels with highest frequencies transfer energy to the middle frequency channels and to the lowest frequency channels, while the middle frequency channels transfer to the lowest channels, this channels only receives energy from the others and do not transfer none. That explains the aspect of the output link spectrum, whose power of the channels decrease as the frequency increases.

In the next figure the maximum power allowable per channel versus the number of channels can be observed in a system with $\lambda = 1.55\mu m$, $\alpha = 0.2dB/km$, $A = 5e-7$ cm² Leff=22km and $\Delta f = 10$ GHz:
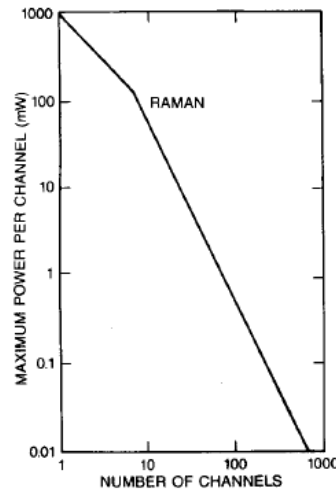
Figure 2.5.9 – Maximum power per channel versus number of channels which ensures SRS degradation below 1 dB for all channels

For systems with several channels the power limit decreases as *1/N* because the Raman gain profile is extremely broad and the powers in all *N* channels contribute to SRS process. As more channels are added, the occupied optical bandwidth increases and the interchannel interactions become more significant and the maximum power per channel decreases as *1/N²* [6].

From the figure 2.5.9 can be seen that to a 100 channels system, the maximum power per channel to the power transfer not occurs is lower than 1mW. The system in study as 1mW per channel and so, some power transfer is seen in figure 2.5.7.

2.6. Conclusions

All the nonlinear effects can be generally categorized as either scattering effects, or effects related to the intensity dependence of the refractive index (Kerr effects). The scattering effects are divided in: stimulated Raman scattering and stimulated Brillouin scattering. The Kerr effects are divided in: Self Phase modulation (SPM), Cross Phase Modulation (XPM), modulation instability, solution formation and four-wave-mixing (FWM). The nonlinear effects increase with the power travelling along the fiber.

The most relevant nonlinear effects to this work are the Cross Phase Modulation and the stimulated Raman scattering. One of the most relevant aspects of Raman scattering is that it extends over a large band of frequencies (approximately 40THz), affecting channels even if they are largely separated.

In a way to analyze some limitations of future technologies like WDM systems, four-wave-mixing was studied, and some ways to minimize its effects were presented. Increase the dispersion of the fiber or use unequal channel spacing in the transmission, proved to be two efficient systems to minimize FWM.

Chapter 3. Modulation Formats

3.1. Introduction

To increase the capacity of optical communication systems, we can increase bandwidth, the number of WDM channels or decrease the channel spacing. But this will bring some limitations caused by the nonlinear effects because more power will travel in the fiber and more channels will interact. Nonlinear effects like self-phase modulation (SPM), cross-phase modulation (XPM), four-wave mixing (FWM), and stimulated Raman scattering (SRS) will appear and to overcome this problems appropriate modulation formats can be used. In an optical communication system the ways to transmit information by an optical signal can be divided in: Intensity Modulation, coherent modulation and differential modulation. In the Intensity modulation the optical signal is codified in two levels of intensity depending if the bit value is a zero or a one. In the case of coherent modulation the signal is transmitted by changing the frequency, the amplitude or the phase of the carrier. The differential modulation is based on phase modulation and use differential encoding of the information. In this chapter we will present a brief analysis of these three different modulated signals. The video overlay signals will be explored also.

3.2. Intensity Modulated signals

In an optical communication system one of the main issues is how to convert an electrical signal into an optical signal. To do that, we can modulate directly the transmission laser or use an external modulator.

A possibility to modulate the signal is to use the intensity modulation (IM). That method is very simple, to represent the logical levels "1" or "0", is just needed to send the signal with high or low strength respectively. The intensity of the logical level "0" does not have to be exactly zero, but the intensity of level "1" must be considerably greater than this intensity. Within the intensity modulated signals two kinds of modulation formats can be found: the return-zero (RZ) and the non-return-to-zero (NRZ).

3.2.1 Non-Return-to-zero (NRZ)

The simplest optical modulation format is the NRZ or often called as non-return-to-zero on-off-keying (NRZ-OOK). In this format the bit occupies the entire temporal slot, so in the case of a sequence of logical 1s, the power of the optical signal does not fall to state zero, and in the case of a sequence of zeros the signal maintains the power low along all sequence.

This modulation format has been the dominant format for optical communication systems. There are several reasons for its use in optical communications. The first one is that, compared with RZ signals NRZ requires a low electrical bandwidth for the transmitters and receivers. The second is that, compared with phase shift keying (PSK) it is less sensitive to laser phase noise. At last it has the simplest configuration for the transmitter and receiver. [13]

The block diagram of a NRZ transmitter is shown in figure 3.2.1.1, where optical signal is modulated with an external modulator which converts the electrical signal into an optical signal at the same data rate. The detection of NRZ signal is made by a

simple photodiode, which converts optical power into electric current. Considering the constant advancements in optical communications, NRZ format may not be the best choice for future high capacity optical networking systems. However, due its simplicity, and historic dominance, this format would be a good reference for the purpose of comparison. [14]
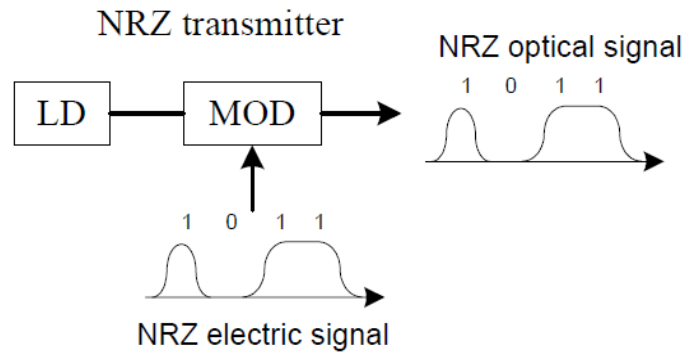
Figure 3.2.1.1 – Block diagram of NRZ transmitter

3.2.2 Return-to-zero (RZ)

In return-to-zero modulation format often called return-to-zero on-off-keying (RZ-OOK) , the bit level "1" does not occupy the entire temporal slot, and the bit power returns to zero before the end of each temporal slot. RZ transmitters can be implemented by the electronic generation of waveforms RZ, and these waves will modulate an optical carrier. Another implementation can be done by generating a NRZ optical signal with an external intensity modulator described above and then the output signal is modulated by a synchronized pulse train with the same data rate as the electrical signal using another intensity modulator as can be seen in the figure 3.2.2.1 [14].
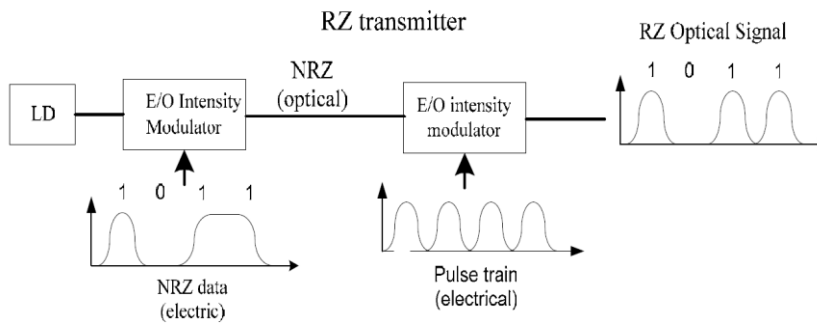
Figure 3.2.2.1 – Bock diagram of a RZ transmitter

3.3 Coherent Signals

In order to improve the limitations present in the base-band signals (this signals cannot be transmitted directly to the most transmission channels because its characteristics are not the ideal to some frequencies ranges) some techniques were defined by increasing the frequencies of these channels, making them match the ideal range of frequencies of the transmission channel. The digital transmission systems, using modulation techniques with carriers, consist on changes the characteristics of a sinusoidal wave along the time.

For simplicity, the electric field of the transmitted signal is considered as a plane wave with the form:

$$E_s(t) = A_s \cos\left[\omega_s t + \phi_s(t)\right]$$

(3.3.1)

Where A_s is the amplitude of the optical signal field, ω_s is the optical signal carrier frequency, and ϕ_s is the phase of the optical signal. To send information, amplitude, frequency, or phase of optical carrier can be modulated. Thus, one of the following three modulation techniques can be implemented: Amplitude shift keying (ASK), Frequency shift keying (FSK) and Phase shift keying (PSK).

3.3.1 Amplitude Shift Keying (ASK)

In this case the transmission is made by changing the amplitude of the carrier maintaining the phase and the frequency of the channels constant. The signal after modulation can be seen as:

$$x_s(t) = A * x(t) * \cos(\omega t)$$

(3.3.1.1)

Where x_s is the signal after modulation, A is the amplitude of the signal, $x(t)$ is the modulating signal, and $\cos(\omega t)$ is the carrier. In the next figure can be seen an example of the signal x_s to a generic bit sequence of "0" and "1":
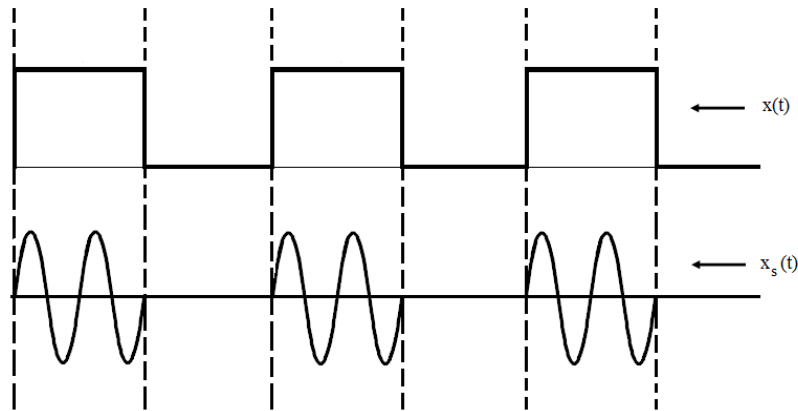
Figure 3.3.1.1 – Evolution of x_s with the signal x(t)

When the signal x(t) as the value "0" no signal appears in the output, when it has the value "1" the output is given by the carrier signal multiplied by the amplitude of the signal *A*.

3.3.2 Frequency shift keying (FSK)

In this modulation format the information is sent in the frequency, maintaining the phase and amplitude of the signal constants. To the different bit values, different frequencies are associated as can be seen next:

If $x(t) = 1$:

$$x_s(t) = A * \cos(\omega_1 t) \tag{3.3.2.1}$$

If $x(t) = 0$:

$$x_s(t) = A * \cos(\omega_2 t) \tag{3.3.2.2}$$

Assuming that $f_1 = f - \Delta f$ and that $f_2 = f + \Delta f$ where Δf is the frequency shift, the expressions (3.3.2.1) and (3.3.2.2) will be given as:

$$x_s(t) = A * \cos(\omega \pm \Delta \omega)t \tag{3.3.2.3}$$

Where the "+" is for the case when bit value is "0" and "−" for the case when its value is "1". Basically this signal can be seen as the addition of two ASK signals with different frequencies. One of them appearing when the bit value is "0" the other one when the bit value is "1". The FSK signal after the modulation can be seen in the next figure:
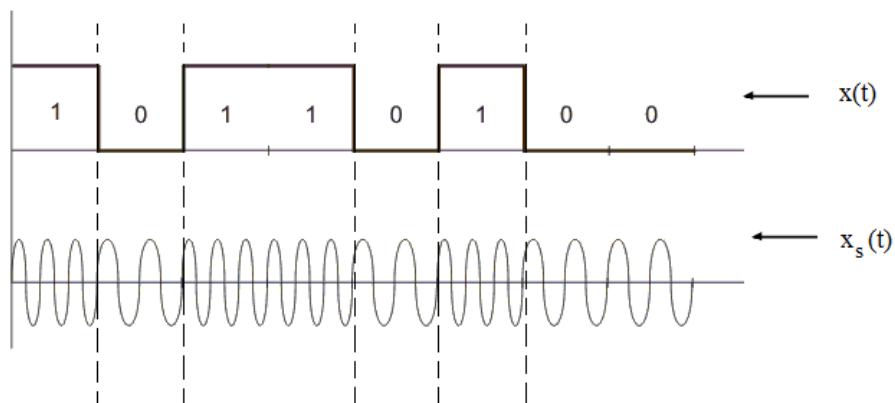
Figure 3.3.2.1 – Modulated FSK signal

This modulation technique has the following characteristics:

- Noise tolerance;

- Higher bandwidth then ASK signals;

37

- The signal amplitude is constant, so its decision level does not have to be adjusted if variation in the received signal occurs;

3.3.3 Phase shift keying (PSK)

In this case is the phase that will change with the modulating signal, maintaining the amplitude and the frequency constants. In this type of signals, two variations can be found: Binary phase shift keying (BPSK) and Quadrature phase shift keying (QPSK). To a BPSK signal the carrier can be given by:

If $x(t) = 1$:

$$x_s(t) = \cos(\omega t)$$

(3.3.3.1)

If $x(t) = 0$:

$$x_s(t) = -\cos(\omega t)$$

(3.3.3.2)

The next figure shows the waveform of a BPSK signal:

Figure 3.3.3.1 – Waveform of a BPSK signal

The quadrature phase shift keying is a multi-phase system based on PSK. In this system two consecutive binary pulses are combined and the four binary pairs are used

to create a sinusoidal wave of high frequency with four phases. The carrier can be given by the next expression:

$$x_i(t) = \cos(\omega t + \theta_i), \text{ i= 1,2,3,4 and } 0 \leq t \leq 2T \qquad (3.3.3.3)$$

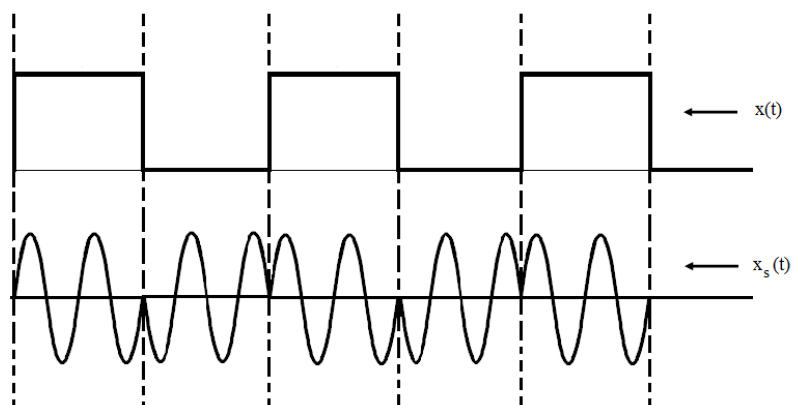The above expression can also be written as:

$$x_i(t) = a_i \cos(\omega t) + b_i \operatorname{sen}(\omega t), \text{ i= 1,2,3,4 and } 0 \leq t \leq 2T \qquad (3.3.3.4)$$

And θ_i can assume the values of:

$$\theta_i = 0, \pm \frac{\pi}{2}, \pi \qquad (3.3.3.5)$$

Or

$$\theta_i = \pm \frac{\pi}{4}, \pm \frac{3\pi}{4} \qquad (3.3.3.6)$$

Sometimes is usual to represent the signals in a form called constellation, where in the horizontal axis is represented the terms in phase ($\cos(\omega t)$) and in the vertical axis the terms in quadrature ($\operatorname{sen}(\omega t)$). The constellations of the signal considering the different phase distributions are given by:
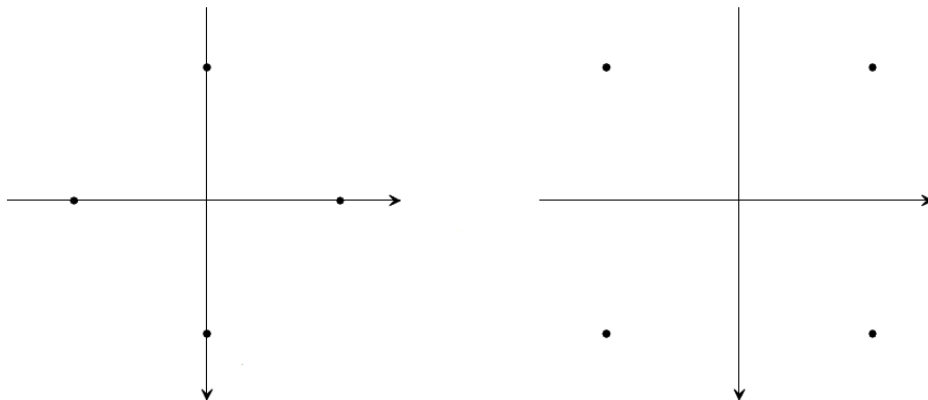

Figure 3.3.3.2 – Signal's constellations: case of phase distribution given by (3.3.3.5) (on the left); and given by (3.3.3.6) (on the right)

3.4 Differential phase modulation formats

3.4.1 Differential Binary Phase Shift Keying (DBPSK)

Differential binary phase shift keying encodes information on the binary phase change between adjacent bits: a 0 is represented by no phase change, while a 1 is represented by a π phase change. DPSK can be implemented in NRZ or RZ format. In NRZ-DPSK the optical power fills completely the slot of a bit, but in the case of RZ-DPSK that does not occur and only a part of the slot is occupied. The main advantage in the use of DPSK instead of OOK comes from sensitivity improvement that can reach the value of 3dB in the limit of high signal-to-noise ratio [15]. That can be easily understood looking at figure 3.4.1.1. In that figure can be seen that the symbol spacing for DPSK is increased by a factor of $\sqrt{2}$ compared OOK to a fixed average power. The energy for each symbol is given by the square of its distance to the origin, and so the average power per symbol is in both cases $x^2/2$. This increase of distance between symbols makes DPSK accept a $\sqrt{2}$ higher deviation of optical noise than OOK to the same BER, which will cause a 3-dB reduction in the OSNR required. This lower requirement of OSNR could be used to increase the transmission distance, reduce optical power requirements, or relax component specifications. [16]

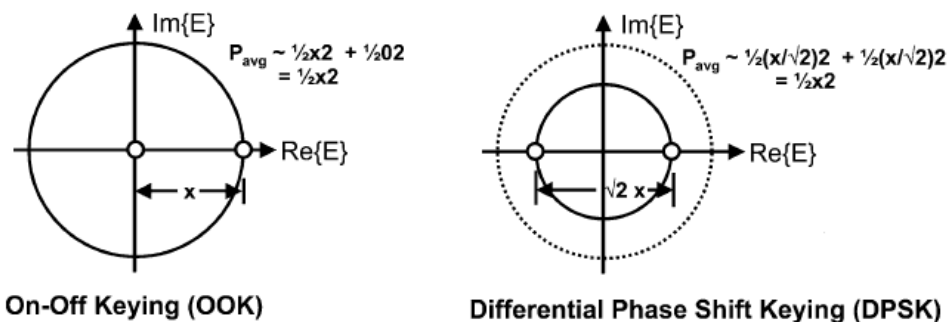Figure 3.4.1.1 – Signal constellation of binary on-off keying (left), and binary phase shift keying (right).

Another benefit of DPSK is that, using balanced detection, it offers large tolerance to power fluctuations in the receiver decision circuit, because the decision threshold does not depend on the input power. DPSK is more robust to narrow-band optical filtering than OOK. DPSK is also more resilient than OOK to some nonlinear

effects because: the optical power is more evenly distributed for DPSK (power is present in every bit slot), which will reduce the bit-pattern-dependent nonlinear effects; other reason is that optical peak power is 3dB lower for DPSK to the same average power [16]. In the transmission, the data signal is first differentially encoded at the transmitter, which avoids error propagation that may occur by differential decoding at the receiver. To perform optical phase modulation a straight-linewidth phase modulator or a Mach-Zehnder Modulator can be used. [15]

3.4.2 Differential Quadrature Phase Shift Keying (DQPSK)

DQPSK is the one of the true multilevel modulation format (more than one bit per symbol) that has received more attention in optical communications lately. It transmits the four phase shifts $\{0, +\pi/2, -\pi/2, \pi\}$ at a symbol rate of half the aggregate bitrate. A DQPSK transmitter is most conveniently implemented by two parallel MZMs operated as phase modulators. In the figure 3.4.2.1 can be seen the corresponding transmitter setup, consisting on a laser source operating continuously, a splitter to divide the light in two paths of equal intensity, two parallel MZMs operated as phase modulators, an optical $\pi/2$ phase shifter in one of the paths, and finally a combiner to produce a single output signal [15] .
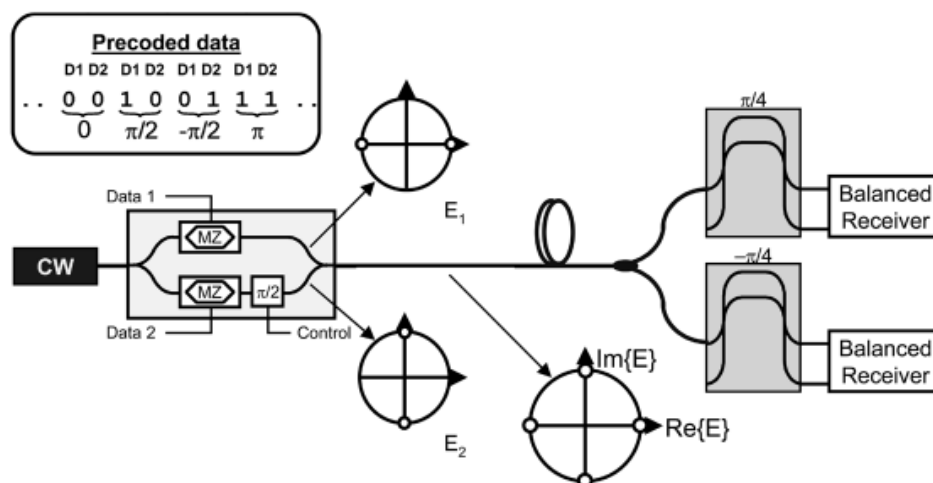

Figure 3.4.2.1 – Structure of a DQPSK system [16]

In the above figure the symbol constellations of both paths are showed as well as the modulator output. The receiver system can be also observed, in this system, the DQPSK signal is first divided in two equal parts, and parallel balanced receivers with differently biased delay interferometers is used to simultaneously demodulate the two binary data streams contained in the DQPSK signal.

3.5 Video Overlay Signals in Passive Optical Networks

One of the main issues in APON deployment is the cost, because FTTH is always more expensive than the metallic networks. One way to overcome this issue is to increase the service revenues, and to do that more services and capacity of the PON is needed. Broadcast video service can bring revenue to this technology. A simple way to provide this service is separate the video signal from the data signal. WDM was selected to insert this third signal into the PON, and the factors that lead to this choice were: it is possible to use EDFAs for video amplification; allows a guard-band between the "basic band" and "enhancement band"; can use the common lasers and filters; and it leaves enough enhancement spectrum. The new wavelength allocation with this service can be seen in the next figure [2]:
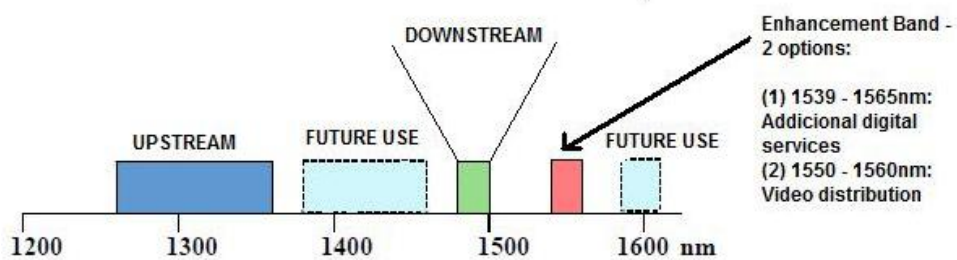

Figure 3.5.1 – Wavelength allocation with broadcast video

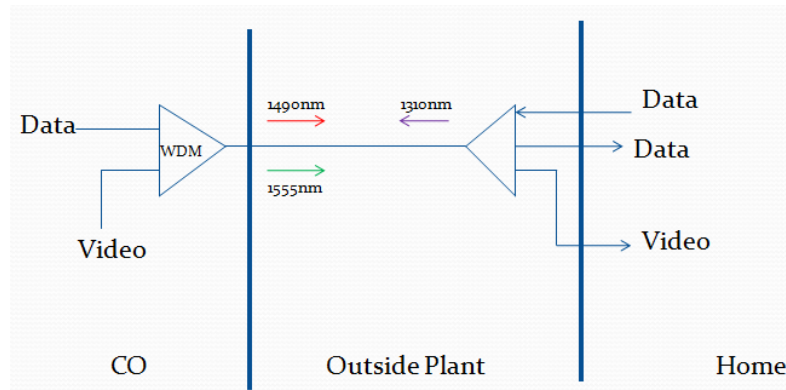The system configuration to this new scenario is seen in the figure 3.5.2:

Figure 3.5.2 – Video overlay system configuration

The modulation format used on video overlay signals is AM-VSB SCM (amplitude modulated vestigial sideband subcarrier-multiplexed), and next a brief description of this modulation will be made.

The spectrum of the base-band signals is symmetric around the central optical frequency, for that reason one half of the signal can be filtered, leaving only one of the sidebands band and preserving all the information. The single sideband (SSB) and the vestigial sideband (VSB) modulations explore this particularity. [17] In SSB one of the sidebands is completely suppressed, in VSB most part of one sideband is transmitted together with a small part of the other band. The advantage of these systems is to spend less power and bandwidth. The disadvantage is that it leads to more complexity of the receivers when compared with the AM systems where the receivers are quite simple. The bandwidth needed to transmit a VSB signal is around 1.25 times higher than to a SSB.

The next figures show a VSB transmission system and the signals evolution along this system. This signal is produced by filtering a double side band signal.
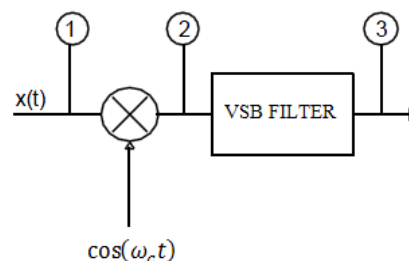

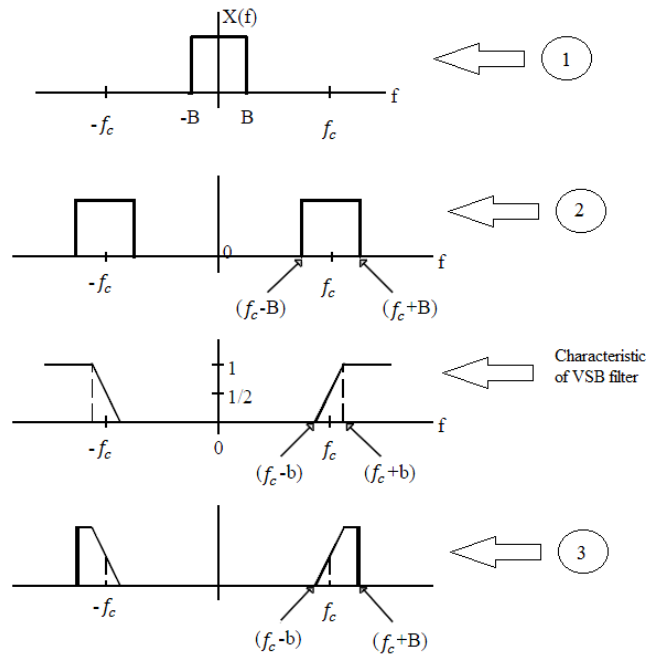Figure 3.5.3 – Transmission system of a VSB signal

Figure 3.5.4 – Spectrum evolution of the signal

While SSB filtering is hard to implement in practice due to difficulties in realizing the appropriate optical or electric filter functions, optical VSB has been successfully demonstrated on NRZ-OOK, RZ-OOK and CSRZ-OOK. In WDM systems filtering can either be done at the transmitter or at the receiver. Filtering at the transmitter provides higher spectral compression and efficiency in WDM transmission. Filtering in the receiver provides lower WDM channel crosstalk if unequal spacing is used [15].

Using 1550 nm for video overlay allows the use of EDFAs to do the amplification, which are relatively cheap amplifiers, a fact that is important in a system deployment, but this also brings some issues. One of the main issues is Raman cross talk between 1490 nm downstream data wavelength and the 1550 nm. Any wavelength plan that puts two wavelengths within 150nm of each other will introduce Raman crosstalk [18]. Due to this non-linear cross talk in the fiber, part of the 1490 nm information is copied onto the 1550 nm wavelength, degrading the video performance [19]. In the G.983.3 situation the power of the pump (data signal at 1490 nm) is around the 0dBm and the video signal power is around the 17dBm. As can be seen in the next figure, the Raman effect has a low-pass characteristic, what makes that the lower channels will suffer worst degradation than the higher channels.
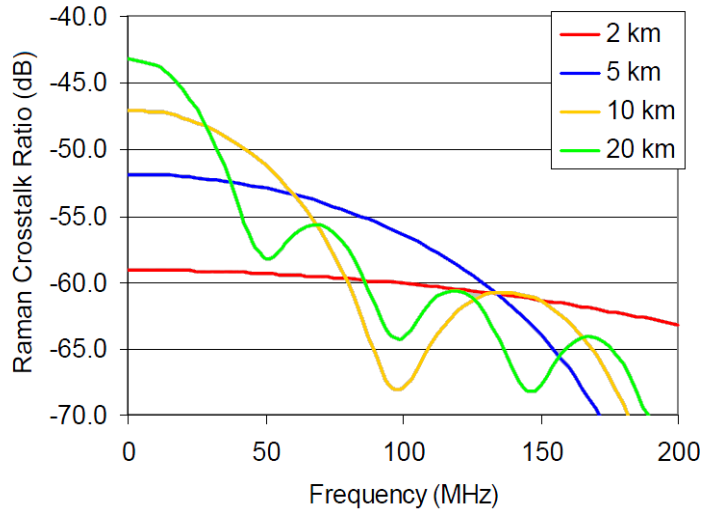
Figure 3.5.5 – Raman Crosstalk Ratio versus Modulation frequency [20]

Raman crosstalk has an important contribution in carrier-to-noise ratio (CNR) degradation, as can be seen in the next expression:

$$CNR = \frac{\frac{1}{2} m^2 I^2}{B_e [i_{th}^2 + 2eI + (RIN + RIN_{Raman})I^2]}$$

(3.5.1)

Where m is the optical modulation index per channel, I the received optical power, B_e the integration bandwidth (4 MHz for an NTSC CATV channel), i_{th} the thermal noise of the receiver, *RIN* the relative intensity noise of the signal without the Raman crosstalk, which is made up of laser *RIN* and added EDFA noise, RIN_{Raman} is the *RIN* generated by Raman crosstalk onto the analog signal [21].

Due to Raman crosstalk behavior for low frequencies, the NTSC channel 2 is the channel with greater degradation. Since the received power and the Raman interference have strong distance dependence, an analysis as function of link distance is next made.

In the next figure can be observed the Raman crosstalk at 55 MHz (frequency of NTSC channel 2) versus fiber length for different wavelength separations:
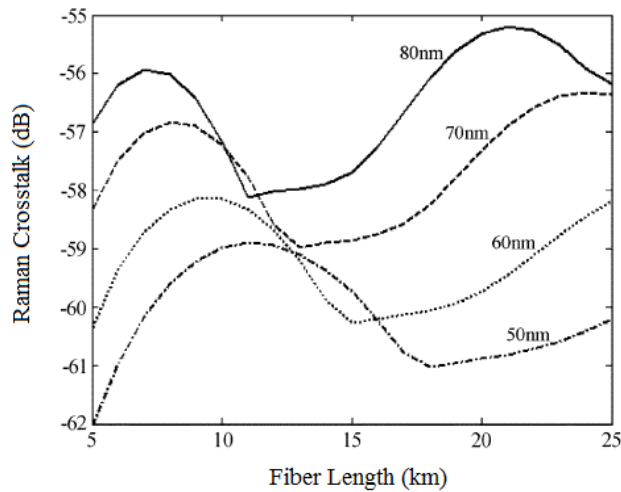
45

Figure 3.5.6 – Raman Crosstalk at 55 MHz versus fiber length for four different wavelength separations [22]

As was seen in the expression 3.5.1 the CNR is dependent of Raman Crosstalk, so it will also vary with fiber length. The resulting CNR curve of a typical G.983.3 system in which the wavelength separation is about 60 nm is showed next:
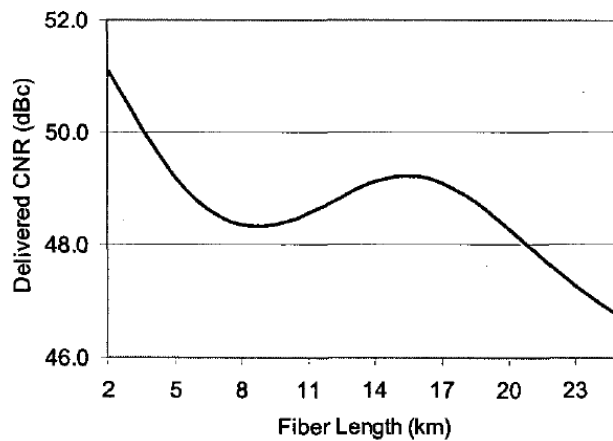
Figure 3.5.7 – CNR performance of a typical G.983.3 system [18]

The above figures show the dependence of CNR with the Raman crosstalk. As the crosstalk increases (fig 3.5.6) the CNR decreases until it achieves the minimum at a distance of about 8 km (fig 3.5.7). For longer distances, dispersion causes phase shift and reduces Raman crosstalk, thus increasing the value of CNR.

Combining some factors, the signal degradation can be even worse, in [21] the authors use 1482 nm for data transmission and 1542 nm external modulated transmitter driven with 80 un-modulated RF carriers for video transmission, with launched power of 3

dBm and 17 dBm respectively. The maximum degradation observed was at the lower frequency channels.

In the next figures CNR of NTSC channel 2 versus fiber length and data launched power can be observed:
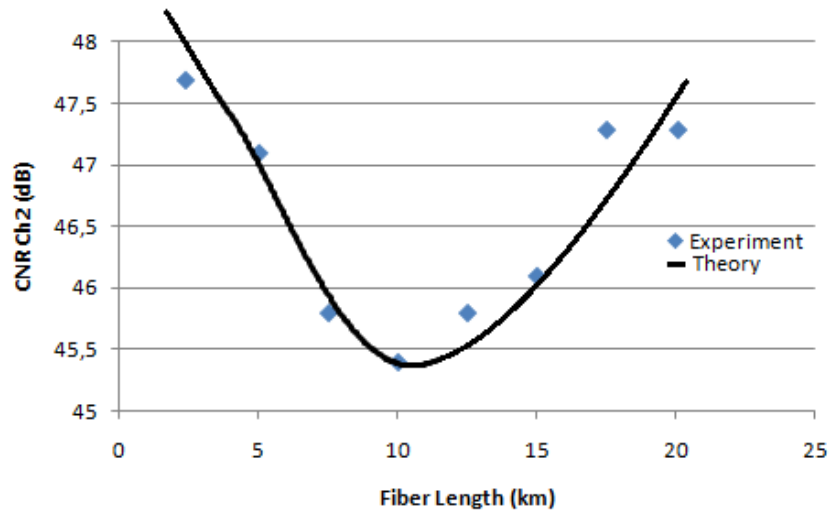
Figure 3.5.8 – CNR of NTSC channel 2 as function of fiber length (based on: [*21*])

Figure 3.5.9 – CNR of NTSC channel 2 as function of launched power of data signal (based on: [*21*])
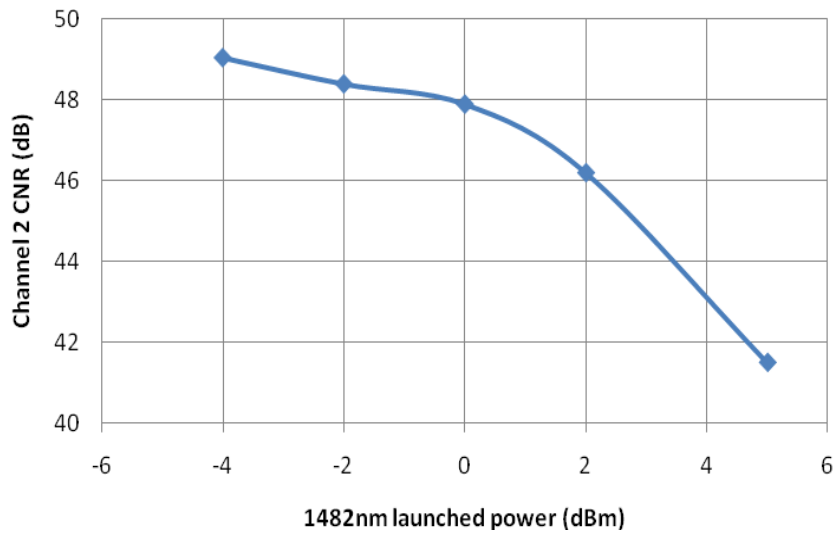
In figure 3.5.8 can be seen that for the worst case (at 10 km) a degradation of up to 3dB can be observed. In figure 3.5.9 as was expected because the data signal works as pump to the video signal, the CNR improves as the data launched power drops.

In this case, can be seen that if the system is used in the limit of the developed standard, the degradation of CNR can be as much as 5 dB for the lowest RF channel. However simple precautions such as, reduce the data launched power, chose adequate fiber length, or make polarization of the signals unaligned, can highly reduce the degradation caused by this effect.

3.6. Conclusions

In this section an overview of the most used modulation formats was made. This section is divided in four major sub-sections: intensity modulated signals, coherent signals, differential phase modulation and video overlay signals in passive optical networks.

Video overlay signals use as modulation format the AM-VSB SCM. In the GPON scenario this signals were multiplexed with data signals and then transmitted at wavelength of 1555nm. When two signals are transmitted at the same time, interactions caused by nonlinear effects will probably appear. These nonlinear effects can cause degradations in both signals. One of the most important effects is the Raman scattering that will cause crosstalk between the data signal and the video signal.

In the next chapter the data signal will be modulated using NRZ and DQPSK with the purpose of studying the crosstalk effects between this signal and the video signal. This will make possible the analysis of the impact of these effects for each modulation format.

Chapter 4. Simulation and results

4.1. Introduction

This chapter deals with the system simulations, and those will be performed with the VPI Systems software [4]. As already referred in previous chapters, the aim is to study the data and video interactions along the optical fibre transmission in the case of PON systems. For the purpose, Carrier-to-noise Ratio (CNR) is used to characterize the quality of the video signal and the Bit error Rate (BER) in the case of digital data signal. Simulation results are presented for various scenarios and the trends and limitations will be interpreted. The chosen modulation formats for the data signals will be: NRZ, QPSK. These formats were chosen in order to observe the most adapted situation and eventual niches for each of them in the scope of PONs, namely, provide some insight in the usage of advanced modulation formats in PONs. For attaining a wider vision, some parameters will be changed, like the wavelength separation of the signals, wavelength band and power of the data signal.

4.2. Interaction between Video and NRZ data channel

Before initiating the study on the interaction between the signals, it is convenient to estimate values of Carrier-to-Noise Ratio (CNR) and Bit Error Rate (BER) for the isolated cases of separate video and data transmission, in order to set conveniently the references. For that purpose the setups shown in figs 4.2.1 and 4.2.2 were implemented using the referred software [4].
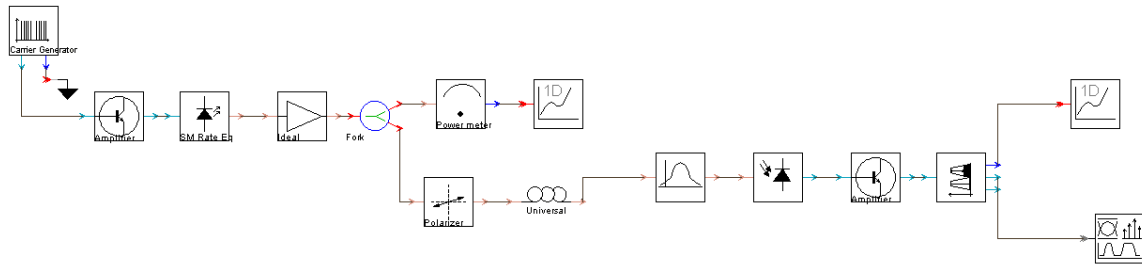

Figure 4.2.1 – Setup to estimate CNR of the video signal
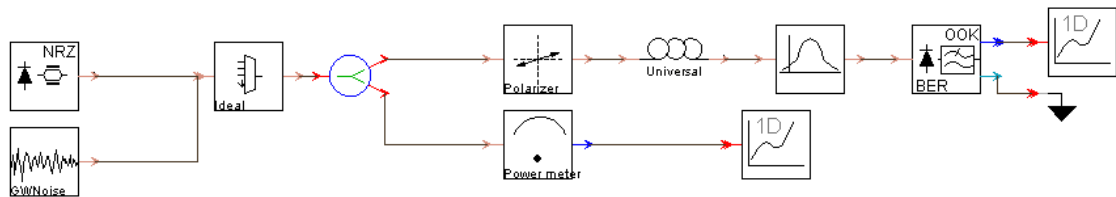

Figure 4.2.2 – Setup to estimate BER of a data signal

In the setup used to estimate CNR of the video signal (figure 4.2.1), 20 video channels are used to modulate the signal intensity of a laser. To set appropriately the power levels, this signal will be amplified and output at approximately 17dBm in a wavelength of 1555nm along a fiber model, referred as universal fiber (see appendix). This model allows separate simulation of the non-linear effects where one can turn them independently on and off. In the present case, FWM and high order non-linear effects are disabled. At the receiver side, the signal will pass through a band pass filter and sent to a carrier noise analyzer. This module, measures the noise of a previously suppressed video channel (in this case channel 18), the power of an adjacent channel, and calculates the CNR of the video signal.

In the setup of the figure 4.2.2, used to estimate the BER of a digital data signal, a NRZ signal is transmitted at approximately 0dBm, with a bit rate of 1.25Gbps, in a wavelength of 1490nm. To this signal a Gaussian-distributed optical white noise source

will be added to provide noise loading. Then, signals will pass through the same fiber of the one used in figure 4.2.1. The reception is made by an optical receiver with BER estimation (estimation method used was the chi-square signal statistics). That module is incorporated by a polarizer, a photodetector, a postdetection low-pass filter and clock recovery circuit. The values obtained for CNR and BER versus fiber length are shown if fig 4.2.3 and 4.2.4 respectively for the two referred signals.
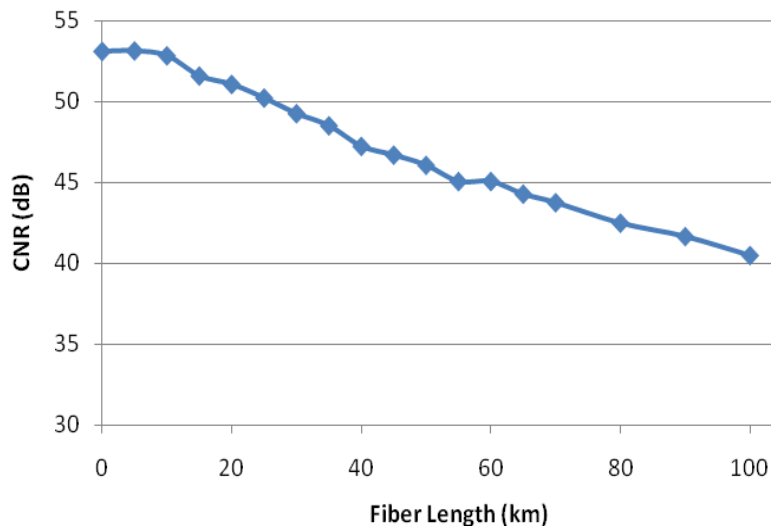

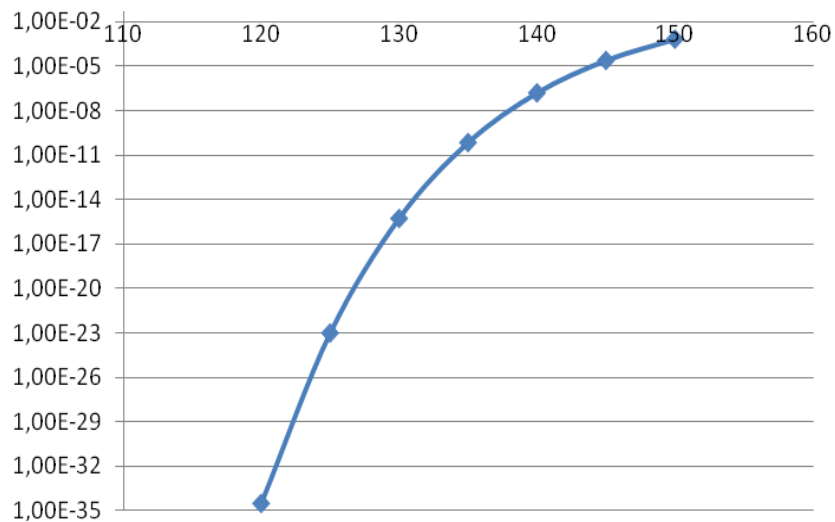Figure 4.2.3 – Video Signal CNR versus fiber length: case of separated transmission

Figure 4.2.4 – Bit Error Rate versus fiber length

In Figs 4.2.3 and 4.2.4 it be seen that, as fiber length increases, BER increases and CNR decreases (so in both situations performance is degraded). As what regards the digital signal fiber propagation it is achieved in error free conditions up to 120 km, which 4.0e-16W/Hz was the injected noise power density.

Both the CNR and BER trends are due to the electrical noise at the receivers, which is constant as opposed to the signal powers that are decreasing due to attenuation.

As referred, 20 video channels modulate the signal intensity of a laser at approximately +17dBm, as is the maximum recommended by G.983.3. This channel is transmitted at 1555nm and will be multiplexed in the fiber with a NRZ data channel at 1490nm. The bit rate of data signal is 1.25Gbps. The setup used is shown in figure 4.2.5:
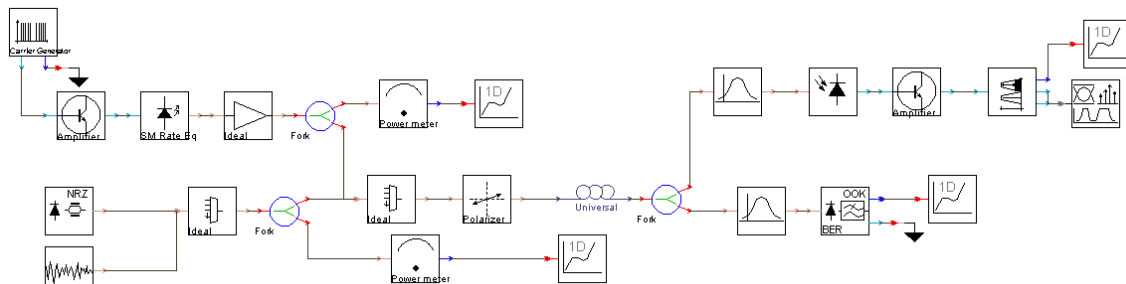

Figure 4.2.5 – Setup of the system to video and NRZ transmission

In figure 4.2.5 the transmission appears on the left side and the reception on the right side. The 20 video channels created by the carrier generator, modulate the transmission laser which is amplified to a power level of 16.94dBm. The data channel is created by a module that simulates an externally modulated laser. This module consists of a CW laser, a PRBS, a NRZ coder, a rise time adjustor (rise time = 1/4/1.25e9s) and a Mach-Zehnder modulator. The output signal is multiplexed together with a noise generator to provide a more realistic BER estimation. Then, the video signal and the data channel are inserted together on the fiber and transmitted to the receiver. In the receiver side, a bandpass filter (with 10Ghz of bandwidth) is inserted and an optical receiver with BER estimator is used for the data signal analysis, and at the output the BER value is read by a 1D numerical analyzer. To estimate CNR of video channel, filtering is made before the detection with a photodiode, and then the signal is sent to a Carrier Noise calculator that gives the Carrier-to-Noise Ratio (CNR) of the video signal.

A data signal at 1490nm with the power of approximately 0dBm and the video signal at 1555nm with the power mentioned above (~17 dBm) are used in the first scenario and only the fiber length is changed. Figure 4.2.6 shows the variation of the CNR versus fiber length.
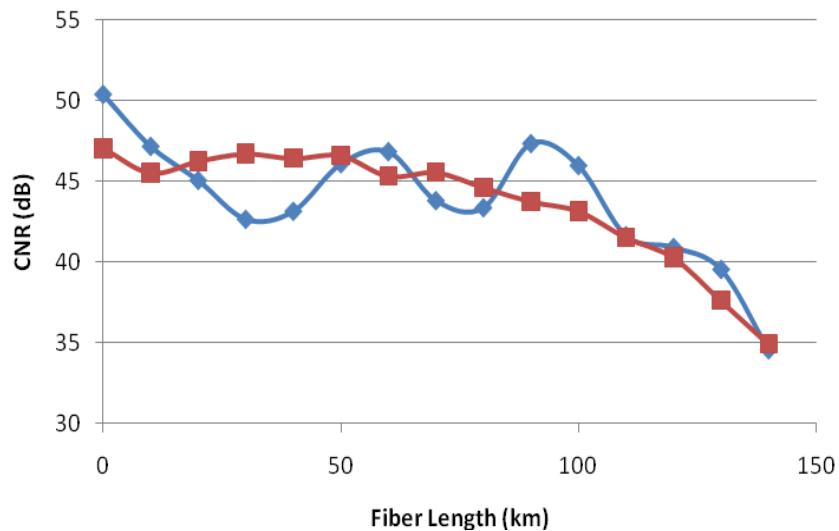

Figure 4.2.6 – CNR for the interaction case of Video signal with NRZ data signal: the blue line is to 16ps/nm/km of dispersion; the red line is to 10ps/nm/km of dispersion

Comparing the results of figures 4.2.3 and 4.2.6, we notice the appearance of signal fluctuations until a fibre length of about 100 km. These, as they are not noticed in fig 4.2.3, may result from nonlinear interaction. It is possible to observe beatings between the carriers due to dispersion and nonlinear effect stemming from the data signal. However, in general terms, signals consistency is noticed since the CNR is approximately 40dB in both cases at 100km. To test the origin of the effect, a simulation was made and is presented with lower dispersion. In this case the fluctuations are less evident almost disappeared. In any case the limitation trends for the video signal are evident and clear.
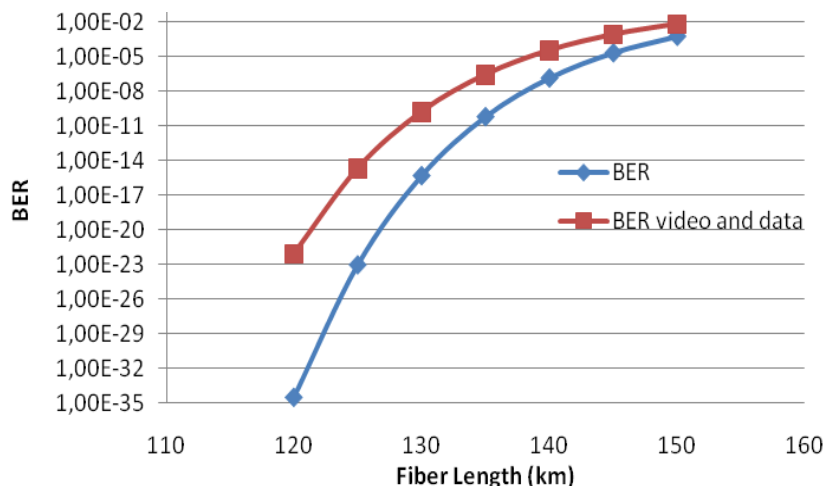
Figure 4.2.7 – BER of data signal versus fiber length: in blue the case of data signal separated from video; in red the case of video and data travelling in the same fiber

From figure 4.2.7 can be seen that the presence of video introduces a penalty, which can be quantified in the loss of 10km in overall reach for a BER limit of 1E-12. That limitation could be explained by the transmission caused by SRS from data to video channel.

In the second scenario as in the previous case, the data signal is transmitted at 1490nm. This signal power is swept. BER and CNR were estimated for two cases: in the presence of a video carrying signal set to approximately 17dBm at 1555nm, and without a video signal. BER values were obtained for 130km fiber and CNR values for 30km fiber. The results can be seen in figure 4.2.8:
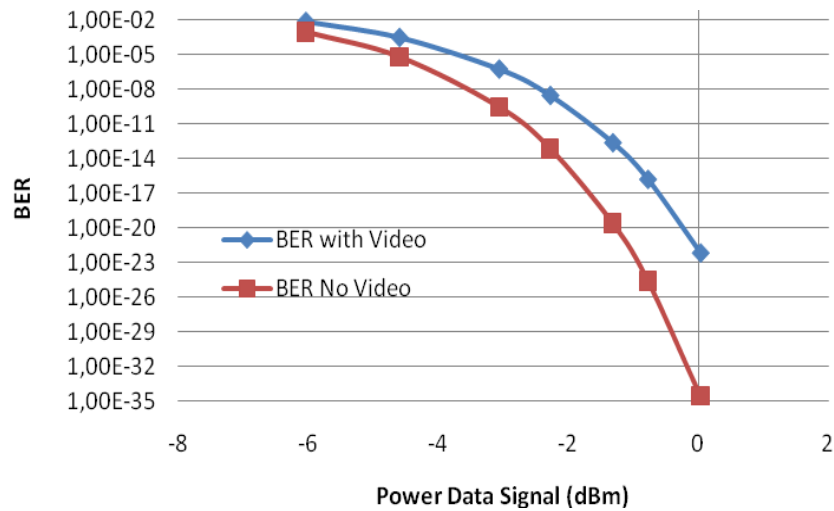
Figure 4.2.8 – BER versus input data power at 130km
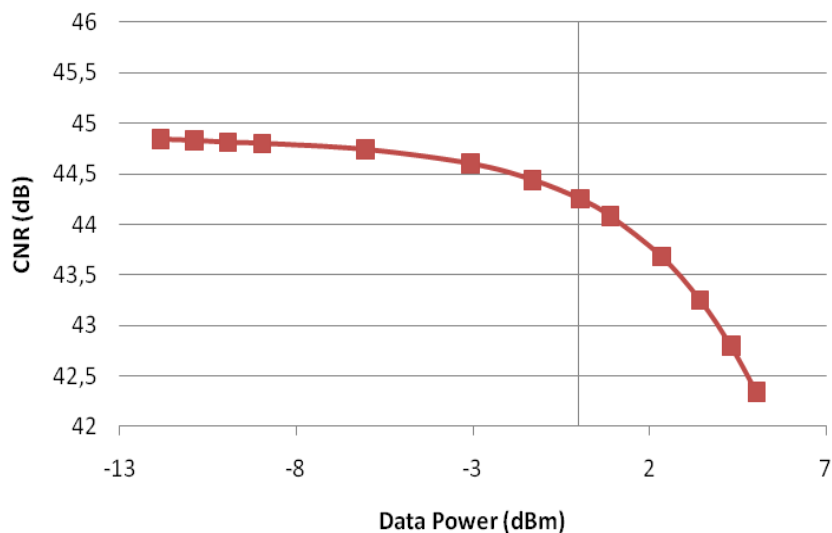
Figure 4.2.9 – CNR versus input data at 30km

In figure 4.2.8 it can be seen that as the data power decreases, the Bit Error Rate increases. That results again from attenuation in fiber. The video introduces a power penalty at BER of 1E-12 of approximately 1dB. In figure 4.2.9 the CNR decreases as the power of data is increased from -12dBm to 5dBm. For low power of the data the impact is low, however as the power grows (>3dBm) the deplection becomes more and more efficient and the CNR decreases asymptotically. This behavior can be interpreted by the scattering generated by the Raman effect. To prove try and validate the idea, both estimations were also performed but in that case with the parameter Raman Scattering off

the universal fiber disabled. In the BER estimation behavior was similar to the case of no video propagation, and in the case of CNR estimation, a constant value (approximately 48dB) was obtained. Note that the CNR was not much penalized (only 2.5dB approximately in a range of almost 17dB of data power swept) because the data powers are too low for produce high Raman Scattering.

In the next scenario the power of the signals is maintained constant as well as the fiber length. Power of data signal is set to ~0dBm, the power of video signal to ~17dBm and the fiber length to 120km. In this case the signal wavelength separation was varied. Data signal was swept from 1450nm to 1515nm and the video signal from 1520nm to 1590nm. The simulation starts with the signals as close as possible (5nm of separation), then the video wavelength is increased to 1525nm, making the separation increase for 10nm. After that, the video was constantly increased by 5nm and the data decreased by the same amount, until a separation of 140nm. BER and CNR estimations were made and the results are shown in the figures 4.2.10 and 4.2.11.
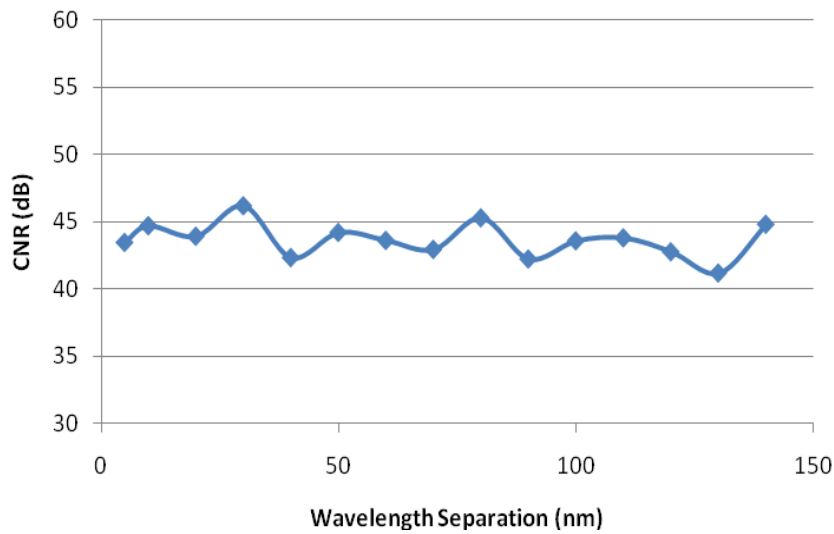

Figure 4.2.10 – CNR of video signal versus signal separation
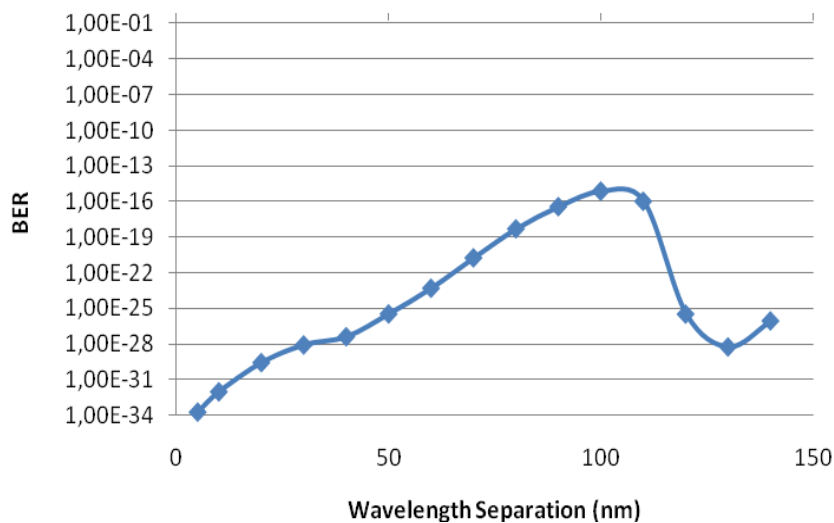
Figure 4.2.11 – BER of data signal versus channel separation

In figure 4.2.11 it can be seen that the Raman scattering effect is present. The waveform is similar to the one of the figure 2.5.1 that represents the Raman gain spectrum, with the peak in to a separation of approximately 100nm. The data signal transfer power to the video signal, acting as pump to that signal. However, the power of data signal is much lower than the video signal, and so, the Raman scattering effect will not be felt much in video performance. The CNR of the video remains practically stable, Fig 4.2.10.

In this scenario, the data signal is sent at 1620nm with the power of ~0dBm and the fiber length is changed. The following Carrier-to-Noise and Bit Error Rate, figures 4.2.12 and 4.2.13 respectively, were obtained:
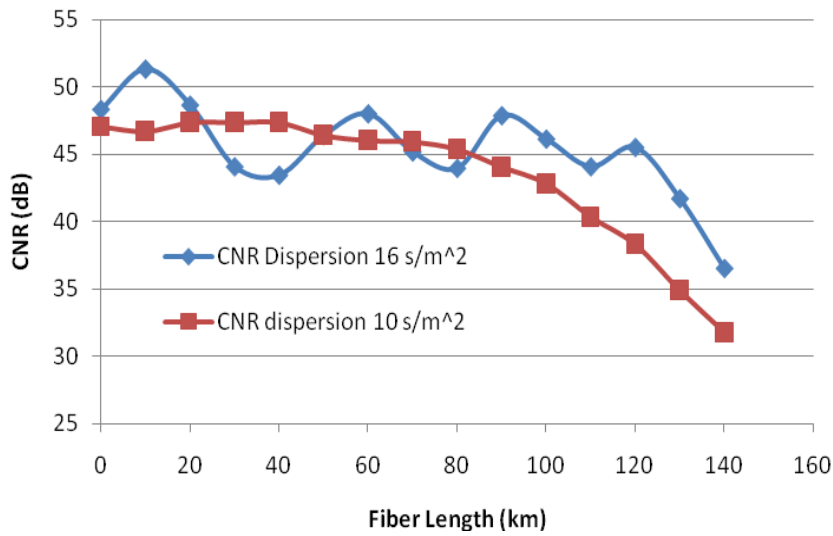
Figure 4.2.12 – CNR versus fiber Length
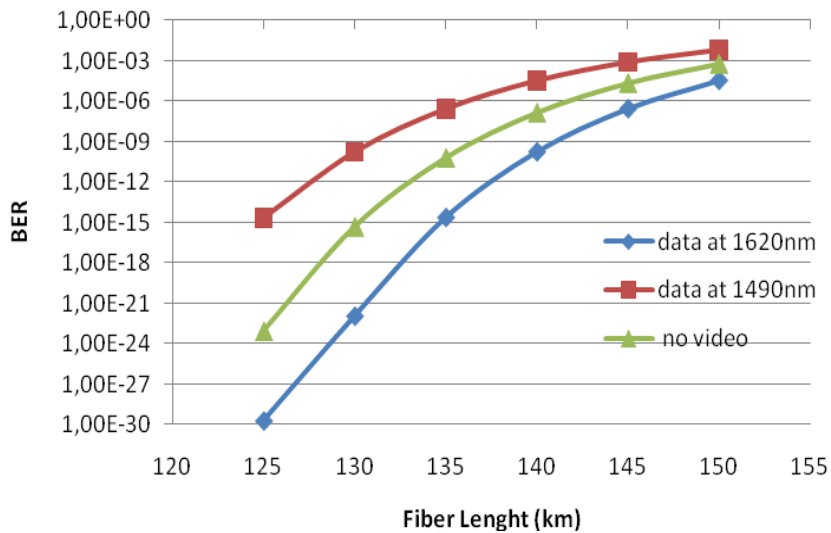
Figure 4.2.13 – BER of data signal versus fiber length to the cases: of data at 1620nm (blue line) and of data at 1490nm (red line)

In figure 4.2.12 the CNR versus fiber length can be seen. Again the oscillations previously spotted were observed and no impact from data was felt. In figure 4.2.13 the BER estimations to the cases of data transmission in 1490nm and in 1620nm can be observed. When the data is transmitted in 1620nm this signal will be amplified by the video signal from Raman scattering effect, and BER values decrease, however when in the 1490, the data will suffer, as already discussed, Raman scattering which will reduce the performance of the data signal when compared to the propagation alone.

Next, the wavelength of data signal will be swept between 1575nm and 1735nm. The wavelength of video signal as well as its optical power does not suffer any modification from the above scenario (1555nm with 16.94dBm). The objective of these measurements is to spot the existence or not of any impact from the Raman effect in the measurements. The results can be observed in Fig 4.2.14 and 4.2.15:

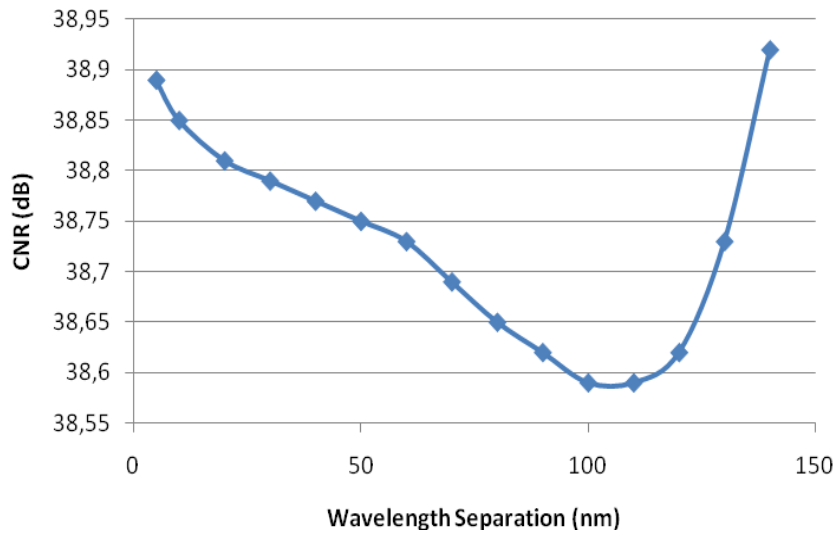Figure 4.2.14 – CNR video signal versus Signal Separation
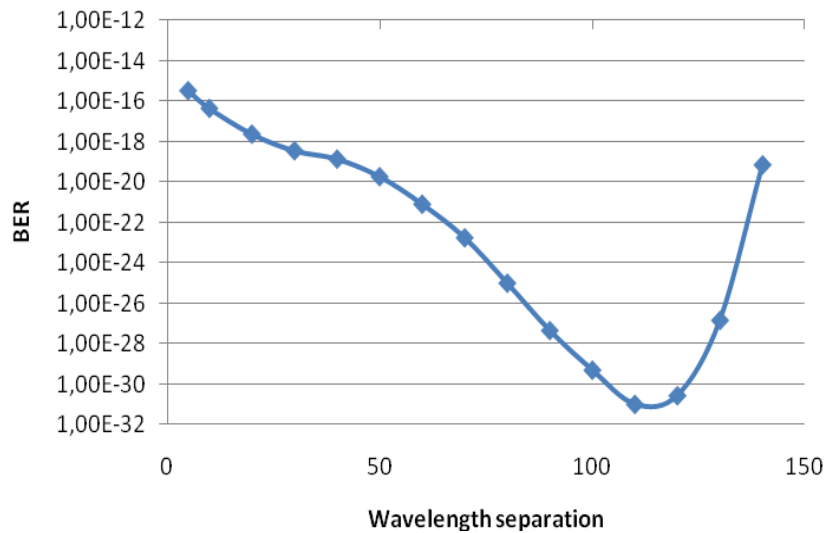

Figure 4.2.15 – BER data signal versus Signal Separation

In these cases is easy to observe the presence of Raman. The CNR will decrease as the separation is increased until it achieves its minimum and then suffers an

improvement from there to the higher separations. However, and in accordance with what was previously said, the changes are minimal (0.3dB). In BER the opposite occurs, it is improved until approximately the same value of wavelength separation and then is degraded. Looking at the figure 2.5.1 that presents the Raman gain Spectrum for a silica fiber, can be seen that its peak is at a separation of about 13THz, that value in wavelength corresponds at around 100nm which is where the minima in figures 4.2.14 and 4.2.15 appear. In this scenario, the transference between video and data will improve the data signal and almost have no effect in the video signal.

4.3. Interaction between Video and DQPSK data signal

In this section the DQPSK (differential quadrature phase shift modulation) is the signal that will be sent through the fiber to interact with the video signal. The CNR and BER estimations will be made for the case of video and data signals respectively.

To start and to have a reference, BER estimation for the case that only DQPSK signal is transmitted in the system. The setup is shown in fig 4.3.1:
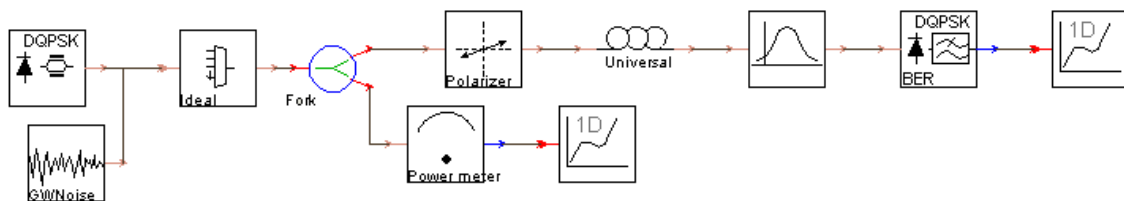

Figure 4.3.1 – Setup of the system to estimate BER of the DQPSK signal

The setup shown in figure 4.3.2 is the one that is used along this section. As in the previous section, 20 video channels will modulate a laser, and a signal of approximately +17dBm will interact with the data signal, which will be in this case a DQPSK signal
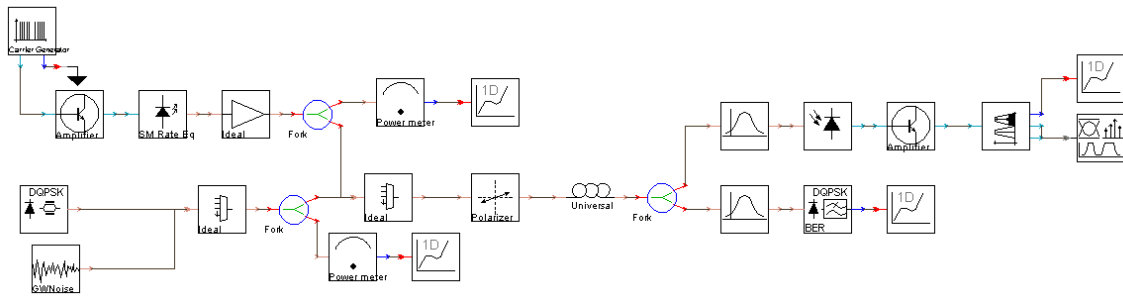
Figure 4.3.2 – Setup of the system to BER and CNR estimation of a DQPSK and a video signal respectively

The system of Figure 4.3.2 is similar to the one of the figure 4.2.5. The differences are the transmitter and the receiver that, in this case, are a DQPSK transmitter and a DQPSK receiver, and the filter bandwidth is changed also (to a value of 5 GHz). The bandwidth of the filter is changed because DQPSK is a narrow band signal, and so narrow filtering must be made, or else huge BER will be presented at the output of the receiver.

In the first scenario the video is sent at 1555nm with an optical power of 16.94dBm and the data at 1490nm with an optical power of 0.02dBm. The only parameter that will be changed along the simulation is the fiber length, which is swept from 0km to 130km. The next results in figure 4.3.3:
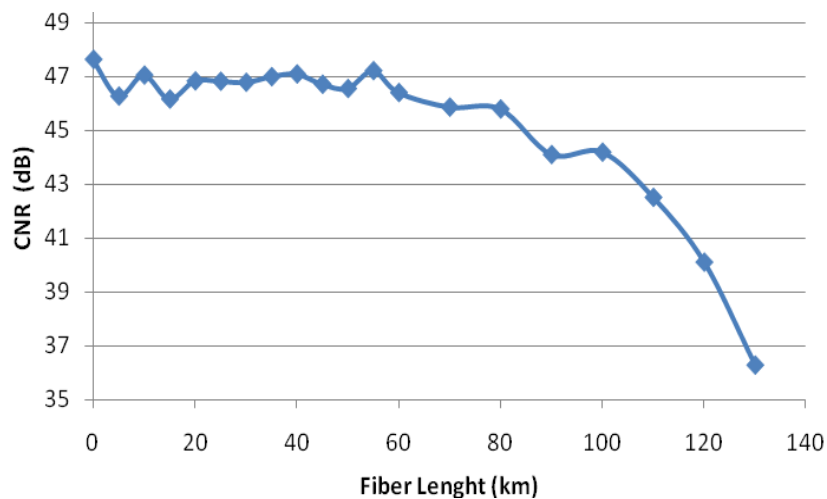
Figure 4.3.3 – CNR of video signal versus Fiber Length
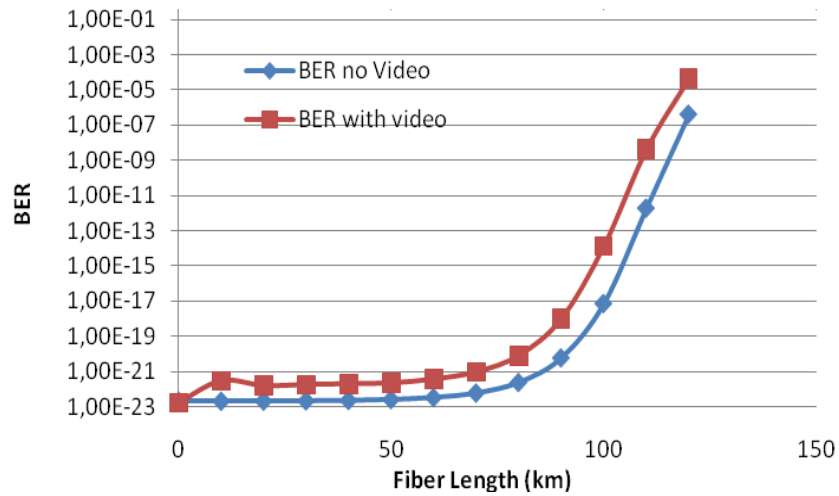
Figure 4.3.4 – BER of the data signal versus fiber length to the case of no video is transmitted (blue line) and to the case of video transmission crossing with signal (red line)

In figures 4.3.3 and 4.3.4, it can be noticed a performance degradation of both video and data signals as the fiber length increases, which is expected by the noise limitations of the receiver

The BER values are better for the case where no video transmission is present. That happens because here the XPM in this case plays also an important role. The data signal is phase modulated therefore cross-phase-modulation will have high impact degrading this signal, figure 4.3.4.

In the following scenario, video and data powers will be maintained (17dBm and 0dBm), as well as the fiber length (50km) and the objective is to study the cross effect as the wavelength separation grows (swept from 5nm to 110nm with the data signal varying from 1465nm to 1515nm and the video signal varying from 1520nm to 1575nm using the same method described previously). The results of CNR and BER are shown in figures 4.3.5 and 4.3.6:
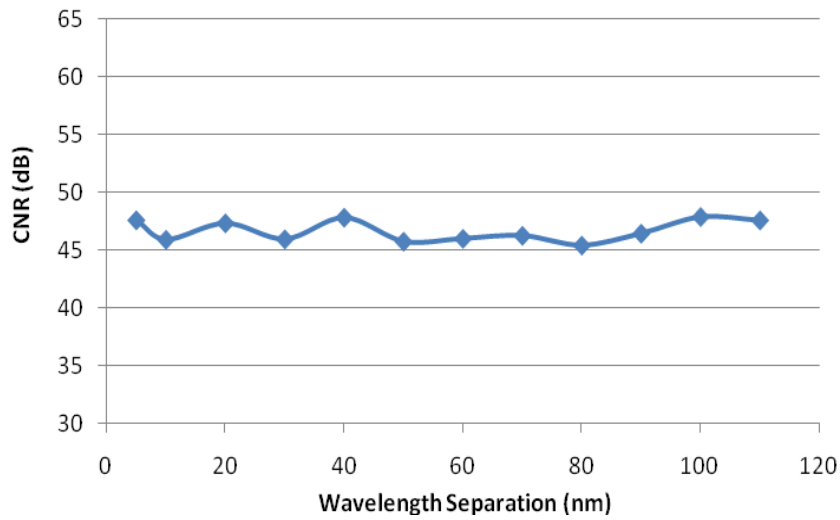
Figure 4.3.5 – CNR of video signal versus Channel separation
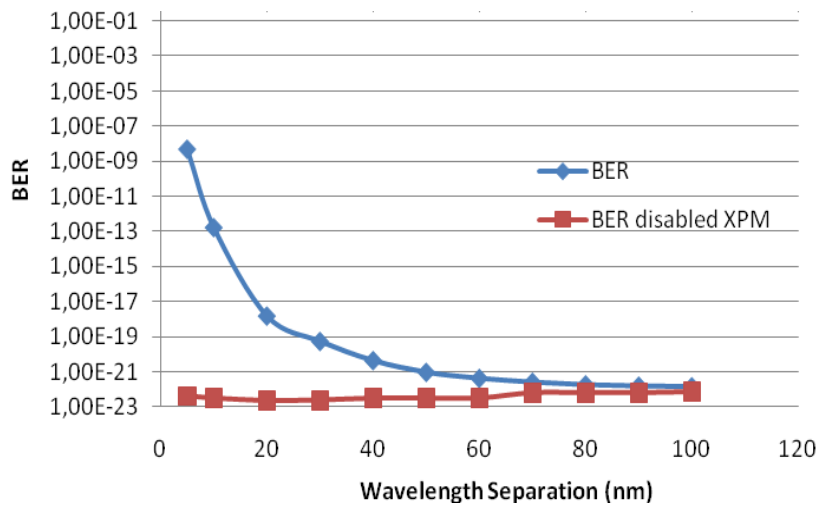
Figure 4.3.6 – BER of the data channel versus Channel separation

In figure 4.3.6 it can be seen that the XPM can affect the performance of the system for lower separation between signals, as expected by the phase matching condition. After 20nm separation the XPM will not be so intense, however its effect is felt until approximately 70 nm of separation. In the figure 4.3.5 the CNR suffers some fluctuations, but it maintains a behavior more or less constant as the separation increases.

In the next scenarios the data signal will be transmitted at lower powers than the video signal, video will be set at 1555nm with 17dBm of optical power and data will

transmitted in above wavelengths. The objective is to study the nonlinear effects for the case of using different bands for transmission. In the first scenario only the fiber length is swept, the data is transmitted at 1620nm at approximately 0dBm. BER ant CNR estimations will be made to this case, and the results can be seen in the next figures.
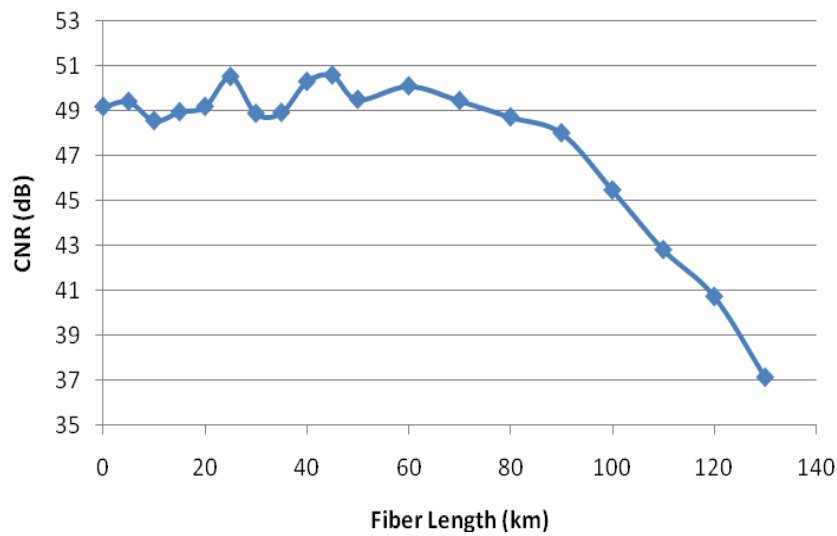
Figure 4.3.7 – CNR versus fiber length to the case of data at 1620nm
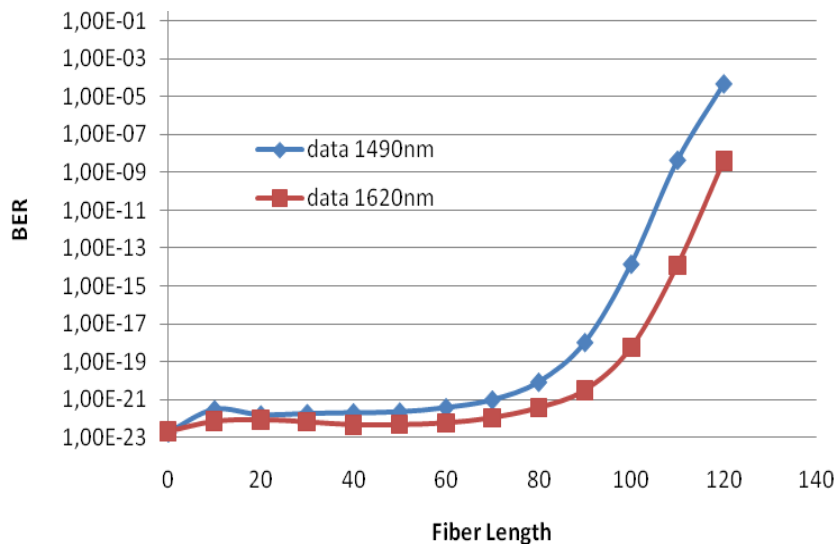
Figure 4.3.8 – BER versus fiber length: red line) data at 1620nm; blue line) data at 1490nm

In the above figures can be seen that the performance of the signals decrease as the fiber length increases. As was seen above, this is due to the noise of the receiver. Both

figures have approximately the same behavior as in the case of data signal at 1490nm, but to the case of data at 1620nm the BER are lower. As seen before, this is result of the amplification provided by video signal from Raman scattering effect.

In the next scenario almost all parameters of the previous scenario were used. The fiber length is constant, 120 km. The parameter changed in this case is the wavelength separation. The CNR and BER estimations can be seen in figures 4.3.9 and 4.3.10.
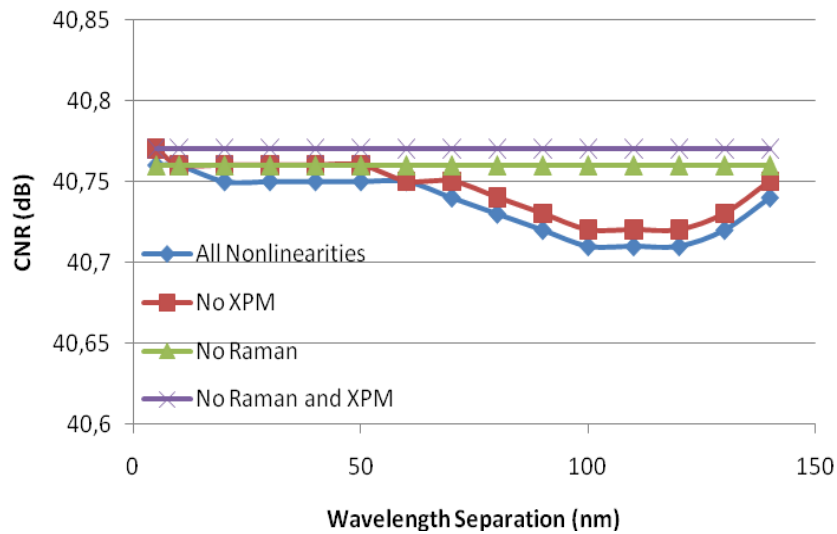
Figure 4.3.9 – CNR versus wavelength separation for the case of data at 1620nm
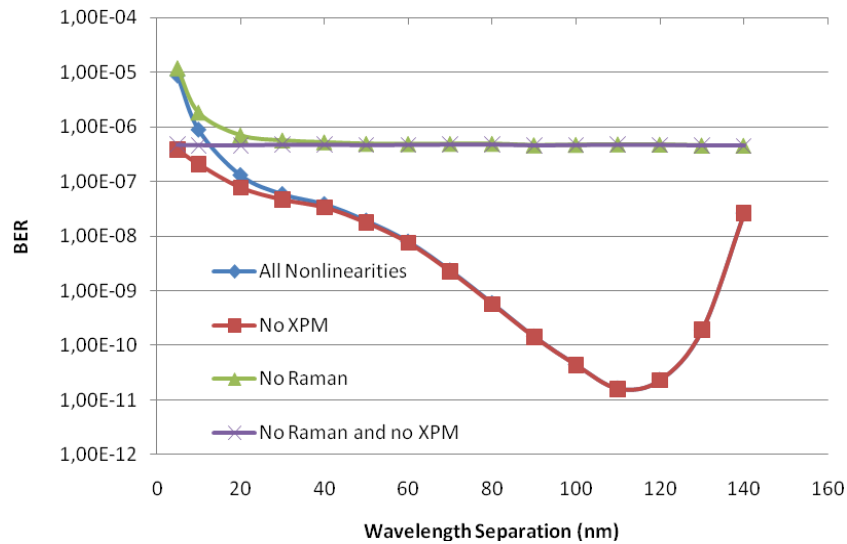
Figure 4.3.10 – BER versus wavelength separation to the case of data at 1620nm

In the figure 4.3.10 can be seen that the XPM can affect the performance of the system. That effect, as in the case of 1490nm, is highly felt for lower channel separations up to 20nm. After this range the XPM will not be felt so intense, due to the phase mismatch, and has a minimal impact after approximately 40nm of separation. In the same figure can be seen the effect of Raman Scattering. In this case, the BER values will suffer a decrease until a value close to the peak of Raman Gain seen in the figure 2.2.4, and then increase again. In figure 4.3.9, can be seen that Raman scattering is felt and the CNR is reduced until a value close to the Raman peak and then increases. However that variation is not that significant (variation of about 0.05dBm was verified).

4.4. Conclusions

In this chapter simulations using VPI software were made to analyze the cross-effects between video and data signal. NRZ and DQPSK signals were used to transmit data signal, and the effects in each signal were analyzed.

In the scenarios using NRZ transmission, the main nonlinear effect observed was the Raman scattering. NRZ is intensity modulated, and any power transference will provide a degradation or improvement in the performance of this signals.

In the case of using DQPSK transmission, the most important nonlinear effect observed was the XPM. DQPSK is phase modulated, and so when the signals are not far enough from each other, XPM is produced affecting the phase, and consequently the performance of the system is degraded.

Chapter 5. Conclusions and future work

5.1. Conclusions

This work has been presented in a set of five chapters. In the First Chapter the context, motivation, structure and objectives, and the main contributions of this work were presented. In the second chapter, an overview of the nonlinear effects is made, and some simulation results are presented to provide a better understanding of its impact in real systems. Cross-phase modulation was studied in a case of a pulse walking through another ten times weaker in a different WDM channel. In this case was possible to observe that the XPM produced will induce broadening in the weaker signal. Another effect observed was the FWM, and the number of FWM products generated by N waves. For example, in a case of 4 WDM channels propagating, 24 FWM products will be generated. These products can highly degrade the performance of a WDM system, and so, two techniques to reduce FWM crosstalk were studied and simulated. The first technique used was increase the dispersion coefficient or eliminate one of the channels. The second one was to use unequal channel spacing. With both techniques it was possible to increase the performance of the system but the second one has the disadvantage of bandwidth expansion that increases with the number of WDM channels. The last effect studied in this chapter was the stimulated Raman scattering. In this case two simulations were performed. The first one shows the case of two signal propagation, and was possible to verify that in this case, the scattering only occurs if the value of Raman threshold is exceeded. In the second simulation, 100

NRZ signals were transmitted. In this system is possible to notice the appearance of SRS effect, which makes the higher frequency channels work as pump the lower frequency channels.

The video signals and its insertion on the Passive Optical Networks deserve special attention in chapter three. The wavelength allocation as well as a system configuration with broadcast video was shown. In this chapter a brief description of some modulation formats was made. Two of these formats were used in the next chapter to transmit data signal.

In chapter four, it was possible to identify the cross-talk effects which are more prejudicial to the actual standards. For NRZ data signals it can be observed that the XPM does not provide a significant degradation. In this case, the Raman scattering is the effect most felt. When the data signal is transmitted at 1620nm, the video signal will work as Raman pump to this signal, and its performance is improved. However, the video signal does not suffer a significant impact (0.3dB only).

In the case of a DQPSK being transmitted as data signal, two effects will be felt, the cross phase modulation, and the Raman Scattering. When the signal separation is low, the XPM due to the video signal will degrade the data signal. When the separation is increased and as it approaches the value of Raman gain peak (at about 100nm), this effect will be more intense and will affect the data signal. Again in this case, the video signal will not be highly degraded by the nonlinear effect, because it adds a much higher power than the data signal.

5.2. Future work

With this work, it was possible to identify and study the main sources of cross talk in PONs. The parameters changed (fiber length, power of data signal, wavelength, and the modulation format) and the effects of those variations in the signals were studied. As the demand of increase the bandwidth will not stop, is important to study the cross effects in future access networks.

The first proposal is to study the same effects for higher data rate signals, the 2.5Gbit/s and the 10Gbit/s systems are most obvious choices, because the first one is already being deployed and the second one is close to practical implementation.

The second proposal is study different modulation formats to understand if they will suffer lower or higher degradation due to these effects. QAM may be an interesting format to study.

The third proposal is to increase the number of data channels and study the case of WDM data systems. In this case, FWM will appear, and could be interesting to observe how this effect will affect the data channels. Observe how the techniques to reduce this effect that were seen above in this work will improve the performance of this systems can be interesting also.

References

[1] ITU-T, "Broadband optical access systems based on passive optical networks," Recommendation G. 984.2, 2003.

[2] ITU-T, "Broadband optical access systems based on passive optical networks," Recommendation G. 983.1, 1998.

[3] Govind P. Agrawal, *Nonlinear Fiber Optics,* Third Edition, Academic Press, 2001

[4] http://www.vpisystems.com/

[5] Bernhard Goebel and Norbert Hanik, *Analytical Calculation of the Number of Four-Wave-Mixing Products in Optical Multichannel Communication Systems,* Technische Universität München, Technical Report, October 2008

[6] Andrew R. Chraplyvy, *Limitations on lightwave Commununcations Imposed by Optical-Fiber Nonlinearities,* Journal of Lighwave Technology, Vol. 8, No. 10, October 1990

[7] Fabrizio Forghieri, R.W. Tkach, A. R. Chraplyvy, *WDM Systems with unequally Spaced Channels,* Journal of Lightwave Technology, Vol. 13, No.5, May 1995

[8] Fabrizio Forghieri, R.W. Tkach, A. R. Chraplyvy, *Reduction of Four-Wave Mixing Crosstalk in WDM Systems using Unequal Spaced Channels,* IEE Photonics Technology Letters, Vol. 6, No. 6, June 1994

[9] Reis, J.D.; Neto, B.; André, P.S; Teixeira, A.T., *WDM Ring Performance Improvement by Means of Four-Wave Mixing Crosstalk Minimization Algorithm,* Microwave and Optical Tech. Letters, Vol. 51, No. 8, pp. 1949 - 1952, August, 2009.

[10] Michael P. Nikodem, Wojciech Żurawsky, Krzysztof M. Abramski, *Four-Wave Mixing in Non-Zero Dispersion Shifted Fibers,* ICTON 2008

[11] Chu Xiang, and James F.Young, *Wavelength shift keying to reduce four-wave mixing crosstalk in WDM,* LEOS 1999, 609-610 vol.2.

[12] S. P. Singh, R. Gangwar, and N. Singh, *Nonlinear scattering effects in optical fibers,* Progress In Electromagnetics Research, PIER 74, 379-405, 2007

[13] Muhammad Haris, *Advanced Modulation formats for high-bit-rate optical networks,* PhD, School of Electrical and Computer Engineering Georgia Institute of Technology, 2008

[14] Sen Zhang, *Advanced Optical Modulation formats in High-speed Lightwave System,* Msc, Department of Electrical Engineering and Computer Science and the Faculty of the Graduate School of the University of Kansas

[15] Peter J.Winzer, and René-Jean Essiambre, *Advanced Optical Modulation Formats for High-Capacity Optical Transport Networks,* Journal of Lightwave Technology, Vol.24, No.12, December 2006

[16] A.H. Gnauck, P.J. Winzer, *Opical Phase-Shift-Keyed Transmission,* Journal of Lightwave Technology, Vol.23, No. 1, January 2005

[17] Clenilson Rodrigues da Silveira, *Estudo de Formatos Especiais de Modulação Digital para Comunicações Opticas,* Msc, Engineering School of São Carlos, of the University of São Paulo, 2009

[18] Michael Aviles, Kerry Litvin, Jun Wang, Barry Colella, Frank J.Effenberg, Feng Tian, *Raman Crosstalk in video overlay passive optical networks,* OFC 2004

[19] Fred Coppinger and David Pichler, *RF Video Overlay in an Ethernet Passive Optical Network,* OFC 2006

[20] Dr. Frank J.Effenberg, *Passive Optical Network Tutorial,* San Diego, CA, USA, OFC2010

[21] F. Coppinger, L. Chen, D.Piehler, *Nonlinear Raman Cross-talk in a Video Overlay Passive Optical Network,* OFC 2003

[22] Feng Tian, Rongqing Hui, Barry Colella, and David Bowler, *Raman Crosstalk in Fiber-Optic Hybrid CATV Systems with wide channel separations,* IEEE Photonics Technology Letters, Vol.16, No. 1, January 2004

[23] Keng-Duan, Guu-Chang Yang, and Wing C.Knowg, *Determination of FWM Products in Unequal-Spaced-Channel WDM Lighwave Systems,* Journal of Lightwave Technology, Vol.18, No 12, December 2000

Appendix

Universal Fiber Module

Description:

The UniversalFiberFwd module is a galaxy (figure a.1) that contains a UniversalFiber. It is a simplified version because it only supports unidirectional flow of the signal − within the UniversalFiber the signal propagates from forward input to forward output. Backward inputs and outputs are not used. This module may be used as a line element − unpumped fiber or pumped in the forward direction.
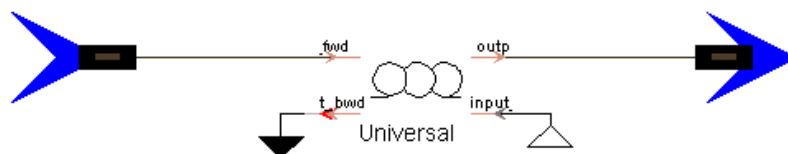

Figure a.1: Implementation of UniversalFiberFwd Galaxy

All the effects presented in the Universal Fiber Model (UFM) are supported, except the effects which need bidirectional data flow:

- Rayleigh scattering;

- Reflectance at event points;

- Brillouin scattering.

As the signals propagate in one direction, the two point boundary value problem (2PBVP) in order to find power distribution of the signals along the fiber is not solved. At the power analysis stage, the signals are only integrated in the forward direction parameter BidirectionalAnalysis in UFM is set to Simplified (refer to Power Analysis for *UniversalFiber*). Amplified noise created due to Raman scattering are considered to be generated only in the forward direction. In this case, a warning message is issued. As the Rayleigh and Brillouin effects are not considered, the distortions are not created. The distortions at the fiber input are treated as if they were PSs, but Raman terms in the power analysis equations are multiplied by a corresponding factor for distortions.

This module supports scalar (PolarizationAnalysis = Scalar) and vector (PolarizationAnalysis = VectorPMD) polarization regimes.

For parameterized signals, the values of a number of physical parameters are saved to the TrackingData (see Chapter 5 of the VPItransmissionMaker™Optical Systems User's Manual). They can be visualized using the LinkAnalyzer module. The fiber parameter GroupRefractiveIndex is used to calculate the fiber delay (TransitTime in LinkAnalyzer).